Climate Change and International Migration*

Mauricio Barbosa Alves — University of Minnesota

Braulio Britos — University of Minnesota

October 29, 2023

Click here to download most recent version

Abstract

This paper studies the impact of climate change on international migration. Using census data from Guatemala, we document novel evidence suggesting that areas affected by a high-heat shock exhibit less migration in the next period. The magnitude is larger in rural areas, where high-heat shocks decrease rural productivity. In the short run, high-heat shocks stop migration from credit-constrained agents needing to pay the migration cost. In this context, climate change's effects are two-sided. While declining rural productivity makes migration more appealing, it also makes it increasingly difficult to pay the migration cost. To analyze these effects, we build a dynamic incomplete-markets migration model with migration costs where high-heat shocks affect rural productivity in credit-constrained households. We then estimate the model to match the high-heat migration link. We show that migration flows increase for different climate change scenarios. Additionally, we find that transfers providing insurance against high-heat shocks decrease migration under all climate change scenarios.

JEL Classification: F22, J61, O11, Q54

*Mauricio Barbosa Alves: barbo104@umn.edu. Braulio Britos: brito032@umn.edu. We thank our advisors, Manuel Amador and Tim Kehoe, for their guidance during this project. We are in debt to Michael E. Waugh for countless hours of dedication. We also want to thank Ricardo Alves Monteiro, Diego Ascarza Mendoza, Nicola Corbellini, Hannes Malmberg, Victor Sancibrian, Todd Schoellman, participants at the Trade and Development Workshop at the University of Minnesota, and UMN-UW Trade-Macro Student Conference. All errors are our own.

1 Introduction

Migration is one of the main adaptation mechanisms individuals have against climate change. By 2050, climate change could lead to more than 216 million internal migrants alone (Clement et al., 2021). Effects are likely to be stronger in developing rural countries, where high heat can cause reductions in crop yields and suitable lands for farming (Mbow et al., 2019). Using census and satellite weather data for Guatemala, we document a negative link between high heat and next year's migration rate to the U.S. We postulate that the mechanism behind this relationship arises from high heat reducing rural productivity and preventing credit-constrained agents from migrating. Under this setting, the effects of climate change are two-sided. The decline in rural productivity generated by climate change impoverishes stayers, making migration more appealing. While on the other hand, it makes it harder for agents to pay the monetary migration cost.

In this paper, we quantify the effects of climate change on international migration flows from Guatemala to the U.S. To do so, we build a dynamic migration incomplete-markets model and estimate it to match our high-heat migration link observed in the data. In our model, agents observe the future decline in rural productivity due to climate change and react to it. At the same time, they are subject to high-heat shocks that translate into lower rural productivity, affecting their income and the possibility of migration. The model predicts an increase in migration once households become aware of climate change. The increase in migration flows is sustained as climate conditions deteriorate. We additionally find strong anticipation effects. Under no anticipation, migration flows in the short run are significantly lower than our baseline, perfect-foresight, case.

Ultimately, we analyze the effects of unconditional cash transfers (UCTs) for two schemes. In the first scheme, we give a transfer to every agent in the home economy. Under this transfer, we find migration flows increasing in most cases, as it helps credit-constrained agents to save and eventually pay the migration cost. In the second scheme, we give a transfer to households that suffered an extreme high-heat shock, defined as a drop in productivity of 40%. We find migration flows decreasing as the transfer helps risk-averse agents to hedge against negative shocks.

A crucial element for our model is estimating the relationship between high heat and migration. For the estimation, we obtain hourly data on temperature for Guatemala at a high degree of spatial granularity. Using this dataset, we compute the number of hours, in days, that temperature is above 30°C (86°F) during

the main crop season for every year. The chosen temperature threshold is aligned with the documented negative effects on crop yields found in Schlenker and Roberts (2009). Finally, we aggregate our measure of high heat at the municipality level to merge it with our census data on migration to the U.S.

We then perform a Fixed-Effect estimation, controlling for municipality heterogeneity, unobservables, and national yearly shocks. The regression results show that when a municipality experiences temperatures above 30°C during the crop season for 24 hours, the migration rate drops by 0.88 migrants per 10,000 people. The coefficient is larger for rural areas compared to urban. In highly urbanized areas, we find no significant effects.

Bazzi (2017) finds a positive relationship between positive agricultural income shocks and international migration in Indonesia. The study highlights how credit constraints limit migration in poor rural areas. Our results align with his findings. Guatemalan migrants face high migration costs of approximately two times the annual average wage.[1] Additionally, the country exhibits low financial inclusion metrics. Only 12.7%, of individuals aged over fifteen, have borrowed from a financial institution or used a credit card; 12.1% have saved at a financial institution; and merely a 10.3% have used a debit or credit card to make a purchase in the past year.[2] To gauge the effects of climate change, we need a model that lines up with the salient features of our data.

We build a dynamic migration model with uninsurable shocks (Aiyagari, 1994) and a non-contingent asset that resembles Lagakos et al. (2023). Every period, households choose between staying and working in the rural sector, or paying the migration cost today and land in the U.S. next period. At home, they are subject to high-heat shocks that affect their effective income. In the U.S., they receive a fixed level of consumption. Apart from the high migration costs, migration does not happen with certainty. We introduce a migration success rate, which reflects how many migrants get detained at the border, and a deportation probability, which represents the likelihood of being deported every period once living in the U.S. In our setting, a high-heat shock decreases the probability of migration. We then estimate the model to build a tight connection between the moment we document from the data and the change in the migration probability the model delivers.

Using crop yield data, we estimate the effect of exposure to high heat on crop yields, obtaining the

[1]The average cost of traveling with a smuggler is between $6000 and $7000 (IOM, 2016).
[2]Data obtained from The Global Findex Database 2021, World Bank, for year 2017

link between high heat and rural productivity. Next, we estimate the model to match the coefficient of our high heat migration link and also the stock of Guatemalan migrants in the U.S. In between, we show that a standard migration model with non-monetary utility costs cannot possibly match the negative link observed in the data. The parameters we estimate are the monetary migration cost and the disutility of living in the U.S. The link we observe is informative about the agents that only migrate in case a good rural shock happens, closely related to the migration cost.

Next, we leverage on temperature projections for different climate change scenarios from Gutiérrez et al. (2021) and construct the distribution of high-heat shocks and their effect on rural productivity shocks for every year until 2100. We fed our model with such projects. In this exercise, we assume that agents have perfect foresight of the exact path of distributions of high-heat shocks and the scenario they are facing. We start from a point where agents are unaware of climate change. In the first period, households learn about climate change, and they start reacting to it.

In our main exercise, we see a substantial increase in the migration flows under all climate change scenarios. By 2040, relative to initial migration, flows increase by 106% in the worst scenario and by 35% in the best scenario. Under climate change, agents foresee a reduction in future income prospects, rendering migration more appeal. In our setting, even with forward-looking agents, migration takes time, as agents need to build up the saves necessary to afford the migration cost.

In a second exercise, we estimate the anticipatory effects of climate change by comparing our main results versus a counterfactual where agents are not forward-looking. The exercise is analogous to the one conducted by Bilal and Rossi-Hansberg (2023). We find migration flows are substantially higher when households can foresee the path of the distribution for high-heat shocks, therefore, the rural productivity distribution. Before the year 2040, migration flows under our baseline scenario are 77% higher than the no-anticipation case for the worst climate change scenario and 30% for the best scenario. When households are unable to observe the rural productivity path, migration increases as they observe and internalize the new distribution of rural productivity. This result is in line with Bilal and Rossi-Hansberg (2023).

Our paper fits in the macro-development literature of migration and occupational choice with credit market frictions (Lagakos et al., 2023; Buera et al., 2020). We abstract from urban agents and model the

rural sector, focusing our attention on modeling intrinsic aspects of migration to the U.S. that migrants must navigate. Additionally, our model introduces uncertainty in migration success and incorporates a deportation risk, presenting an additional layer of risk migrants bear.

The main contribution of our paper is the estimation of the climate change effects on international migration in a developing country. Research such as Bilal and Rossi-Hansberg (2023) studies the effects of climate change in a spatial migration model but is limited to within the U.S., as in Caliendo et al. (2019), where climate change affects amenities and local depreciation rates of capital across the U.S. Our model differentiates from theirs as we abstract from capital and non-monetary migration costs to take into account household heterogeneity, credit constraints, asset holdings scarcity, and monetary migration costs, which are salient features of developing economies. Also, our reduced-form estimations contribute to the literature on weather events on migration (Bazzi, 2017; Cattaneo and Peri, 2016; Jessoe et al., 2018).

2 High Heat and Migration

In this section, we show the negative link between high heat and migration, how the link is stronger in rural areas, and what is the mechanism behind this relationship. We will use the resulting reduced-form coefficient from our regression as an input to estimate the structural model we build in the next section. Now, we proceed as follows. First, we describe the dataset that we use to estimate the impact of high heat on migration flows. Second, we provide details about the reduced-form formulation for the estimation and discuss the results. Third, we show the estimate the effects in rural areas and discuss the mechanism behind our findings.

2.1 Data

Our dataset is of two types. The first is household-level microdata from Guatemala's most recent national census, conducted by the National Statistical Institute (INE) in 2018. In this dataset, we observe migration decisions from previous household members who currently reside abroad and migrated during the 2002-18 period. The second dataset corresponds to satellite weather data. We extract hourly land temperature observations at a high-resolution raster from Copernicus Climate Change Service (2019) for the 1950-2022

period. Next, we provide more details on both datasets and the construction of our variables of interest.

Migration data. Our primary dataset utilized for our analysis is from the "XII National Population and VII Housing Census 2018". This comprehensive dataset incorporates information about international migrants who left their households between 2002 and 2018. Most importantly, the dataset provides details about the geographical location of each household down to the municipality level, as well as the destination country for each emigrant. This level of detail enables us to determine migration flows from specific municipalities to international destinations.

We compute the municipal migration rate as the total of international migrants from rural households in a specific year and then divide it by the total rural population, as reported in 2018. We calculate it for every year and municipality. In our estimations, we consider only migration coming from individuals between 15 and 65 years of age, as these migrants are mainly incentivized by economic reasons.

Satellite temperature data. We employ hourly average land temperature data at the raster level of 0.1° by 0.1°[3] and calculate the number of days of exposure to temperatures above 30°C/86°F. For example, in case hourly temperatures exceed 30°C for 6 hours, this counts as 0.25 days of exposure. We then aggregate exposure over the main crop season[4] to obtain the total number of days of exposure for that raster. To match our raster-level exposure data with our municipal-level data, we calculate exposure's weighted municipal average over the rasters that are partially and completely contained in the municipal boundary. We weigh the rasters by area and the 2010 value of total crop production using satellite data from International Food Policy Research Institute (2019).[5]

We select 30°C as our temperature threshold based on the negative effects of exposure to this temperature on crop yields documented in Schlenker and Roberts (2009). Their paper finds non-linear temperature effects for maize, cotton, and soybean yields. We are interested in estimating the effect of high heat through rural productivity on international migration.

[3] Roughly 11 by 11kms, or 6.5 by 6.5 miles.
[4] For Guatemala, the main crop season goes from April to September (World Food Program, 2015).
[5] The size of this weighting raster is 0.083° by 0.083°, smaller than our weather raster.

2.2 Reduced-Form Estimates

Our paper focuses on the effect of high heat on migration through rural productivity. The spatial granularity of our data allows us to estimate the effect on migration, taking into account heterogeneity in municipalities and aggregate shocks. Consequently, we use a Fixed-effects estimation. Our approach enables us to account for municipal differences in weather and migration flows. It also controls by time-invariant observed and unobserved municipal factors. These factors can include elements like the degree of violence, political instability, economic conditions, infrastructure, environmental factors, land quality, cultural aspects, and more. We also include a year fixed-effect term to control for national aggregate shocks specific to the year. Our baseline specification is the following

$$y_{mt} = \beta_e Exposure_{mt-1} + \alpha_m + \eta_t + \varepsilon_{mt} \tag{1}$$

Where y_{mt} is the rural migration rate at the municipality-year level; $Exposure_{mt-1}$ is the number of days during the main crop season a municipality has been exposed to temperatures above 30°C/86°F for the previous year; α_m and η_t are the fixed effect terms for municipality and year respectively; ε_{mt} is the error term.

We introduce the lag of our temperature variable rather than its contemporary value, largely due to the timing of the main crop season in Guatemala, which goes from April to September. Given we are interested in estimating the effect of a bad crop on the migration flows, using contemporary values might be misleading. First, our migration data is annual; second, the harvest happens in September. Additionally, the migration decision precedes the actual move. Given the cost of migrating to the U.S., households might need time to gather resources and make necessary arrangements before migrating. On a second specification, we show that the effect of the contemporary value is lower than the lagged. Furthermore, we add a specification controlling for departmental[6] aggregate shocks specific to the year. These terms clean for unobservable and observable aggregate year changes at the department level, such as fluctuations in violence, income, and weather, among other patterns.

Our main estimator is β_e. This value captures the change of an increase in the duration of exposure on the migration rate of the following year. Given an increase in the number of days, a negative coefficient

[6] In Guatemala, a department is an administrative region that is above the municipality. There are twenty-two in the country.

represents a reduction in the municipal migration rate. Lastly, we compute robust standard errors to account for the inherent heteroskedasticity in such models.

Table 1: Exposure on Rural Migration Rate

Variables	(1) Rural Mig. Rate	(2) Rural Mig. Rate	(3) Rural Mig. Rate
Lagged Exposure	-0.880***	-0.762***	-0.426**
	(0.152)	(0.132)	(0.182)
Contemporary Exposure		-0.405***	
		(0.090)	
Constant	8.964***	10.156***	7.779***
	(0.753)	(0.720)	(0.925)
Observations	5,236	5,236	5,236
R^2	0.263	0.264	0.545
Number of Municipalities	309	309	309
Time and Municipality FE	YES	YES	YES
Department x Time FE	NO	NO	YES

Note: The table shows the effect of exposure on the rural migration rate across several specifications. FE stands for Fixed-Effect. Robust standard errors are in parentheses. *** p<0.01, ** p<0.05, * p<0.1

Results are reported in Table 1. As we can see, the coefficients are negative and significant. Going to the first column, an increase in lagged exposure decreases the municipal rural migration rate by 0.88 migrants in 10,000 rural inhabitants. In our second specification, we find the effect of lagged exposure to be roughly the same as in the first specification. The effect of the contemporary value of exposure is lower than its lag and significant. Finally, our third specification shows the same relationship, but the magnitude decreases. Ultimately, we find across the three specifications, a persistent negative link between high heat during the crop season, and international migration flows.

In order to comprehend this negative link, we run our baseline Fixed-effects specification in (1) by categories of municipalities according to their percentage of rural population. We summarize our results in Figure 1.[7] We plot our point-estimate value for β_e; the grey band represents the 95% confidence interval. From the graph, we can see how the effect of exposure on migration is larger and more significant for municipalities in rural areas. For urbanized areas, the effect is not significant and close to zero. This

[7]Further details about the regression results can be found in Table A.2 of the Appendix.

outcome suggests that elevated temperatures affect migration decisions in rural households more than their urban counterpart.

Figure 1: Effect of Exposure on Migration Rate by Percentage of Rural Population

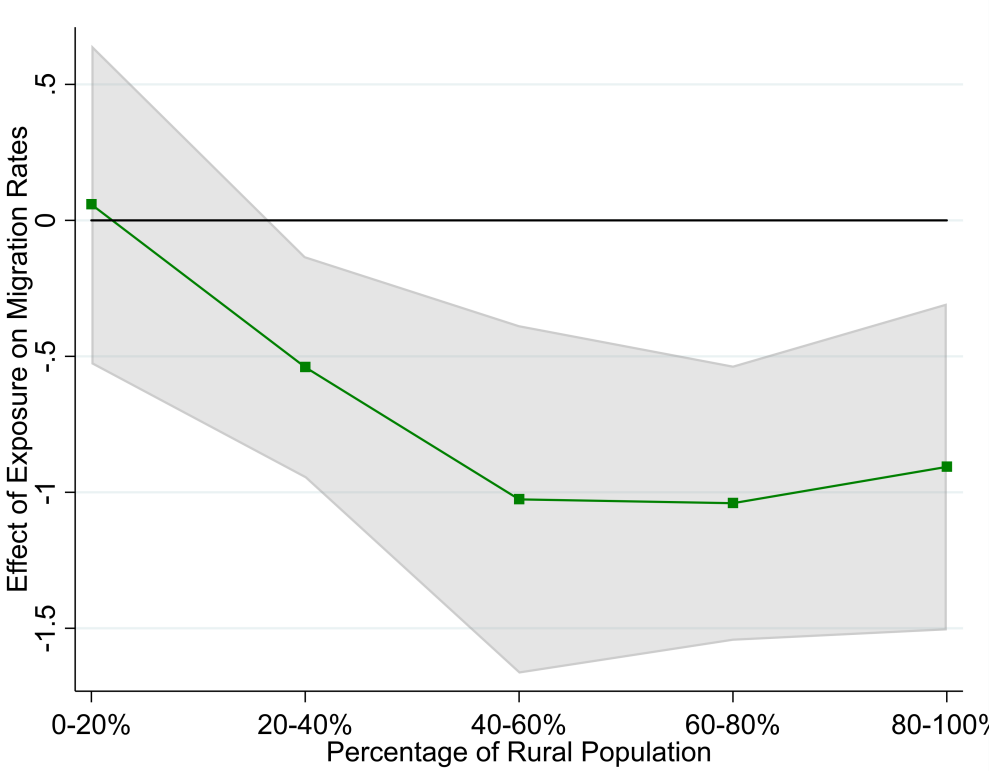

Note: The plot shows the coefficients of lagged exposure from specification (1), for different samples of municipalities according to their share of rural population. In particular, we created five bins following the percentage of rural population each municipality has. We report the point-estimate for each bin in green, and the 95% confidence interval in gray.

Our findings seem to align with Bazzi (2017). Our interpretation of the results is that when a household experiences a high-heat shock, it leads to a decrease in rural productivity, and with agents facing credit constraints and high migration costs, fewer agents will be able to pay the migration cost, making the municipal migration rate decrease.

Leveraging on a similar mechanism to the one we propose, Amirapu et al. (2022) exploits extreme high-heat variation over time and space to study political participation in India. Their main hypothesis is that high heat depletes crop productivity. They find a stronger effect in rural areas, consistent with our findings for Guatemala.

Finally, we do a similar exercise estimating the effect of exposure on rural migration for different temperature thresholds. Results are shown in Figure A.1 of the Appendix. As we can observe, the

effect on migration rates is higher for exposure at higher temperatures. This result seems to align with the non-linear effects of temperature exposure found for crop yields in Schlenker and Roberts (2009). Although the coefficients are significant with respect to zero, we cannot confirm that there are significant differences in the coefficients.

3 A Model of Migration and High-Heat Shocks

In this section, we describe our dynamic migration model, building on the work of Lagakos et al. (2023). Our model is able to match the negative short-run link between migration and high-heat shocks. In our setting, agents are subject to income shocks due to high-heat conditions that affect rural productivity. Every period, agents can choose to stay and work in the rural sector or migrate to the U.S. Agents choosing to stay are able to save to smooth uninsurable income fluctuations, as in Aiyagari (1994), and/or to migrate eventually. Those choosing to migrate pay a monetary migration cost today and arrive in the U.S. the next period, subject to being detained by immigration authorities. Once in the U.S., the agent receives a fixed level of consumption every period but is subject to deportation. Finally, we model climate change as changes in the distribution of high heat along a transition, making rural yields decrease over time. Next, we proceed to describe the setup in more detail.

3.1 Model Setup

Preferences. The economy is populated by a continuum of agents that are infinitely-lived. Agents maximize expected utility over their lifetime with a discount factor of $\beta \in (0,1)$. There is a single consumption good, and they have constant relative risk aversion preferences:

$$u(c_t) = \frac{c_t^{1-\sigma}}{1-\sigma} \tag{2}$$

where σ is the relative risk aversion coefficient. Migrants living in the U.S. receive a constant level of consumption c^* and a disutility cost ν multiplicative to utility, making $u(c^*)\nu$ the period utility of being in the U.S. c^* captures the consumption gap between Guatemalans in the U.S. and agents in Guatemala, while ν represents the non-monetary costs of having to be away from family and adapt to new rules and

language, among others.

Agent Productivity. Each agent at home is endowed with time-invariant rural productivity η, drawn from a log-normal distribution: $\ln(\eta) \sim \mathcal{N}(\mu_\eta, \sigma_\eta)$. In our setting, agent productivity is the efficiency units an agent provides labor. An increase in σ_η implies a higher dispersion in rural productivity and, as we will see next, agent income. The agent's productivity at home does not affect the consumption level or earnings in the U.S.[8]

Production. There is a continuum of competitive firms employing labor. Their production function is $Y_t = L_t^\alpha$, where L_t is the number of efficiency units employed, and α is the returns to scale parameter. The firms pay the agents w_t for every efficiency units of labor.

Income and High-Heat Shocks. Every period agents at home work, providing η units of labor, and receive a transitory high-heat shock z_t that is uninsurable and iid across agents (Aiyagari, 1994). z_t is the effect of high heat on rural productivity. Effective hours are then given by

$$\ell(\eta, z_t) = \eta z_t \tag{3}$$

With wages equal to w_t per efficiency units, we have that labor income is $w_t \ell(\eta, z_t) = w_t \eta z_t$.

We further assume z_t has the following form

$$\ln(z_t) = \ln(1-\chi) \times h_t \tag{4}$$

where χ is the drop in rural yields by one complete day of exposure, and h_t is the number of hours of exposure above 30°C, in equivalent days. Further details about the distribution of exposure are provided in Section 4.2.

Savings. Agents at home are able to save in a risk-free asset a. The asset's price is given by $q > \beta$, which is exogenous in our model. We assume agents cannot borrow, meaning asset holdings must satisfy $a \geqslant 0$ at all periods. In addition, we assume agents can choose the asset holdings in a grid $\mathcal{A}$. In Section B of the Appendix, we provide further detail about this approach.

[8] One interpretation is that the agents have access to labor income that is independent of their rural productivity in the home economy, such as knowing techniques and inputs useful for production in the home economy but not in the U.S. Additionally, in the literature Adamopoulos et al. (2022) calibrates the correlation between agricultural and non-agricultural abilities to find this correlation to be 0.289.

Migration. Besides savings and consumption, agents have the option to migrate. Every period, the agent decides either to stay and work, or pay a monetary migration cost m^e and migrate to the U.S. In the case the agent chooses to migrate, it is subject to an exogenous probability of successfully migrating of $\phi \in (0, 1]$. Migration is permanent unless the agent gets deported. With probability $(1 - \phi)$, the agent is sent back to the home economy. In our model, ϕ represents the probability of an agent successfully arriving in the U.S. and evading immigration controls at the border. Furthermore, we assume the agent cannot bring assets into the U.S.

We follow the recent quantitative literature on migration (Caliendo et al., 2019; Lagakos et al., 2023; Bilal and Rossi-Hansberg, 2023) and include idiosyncratic taste shocks to the migration decision. Every period, each agent receives a pair of shocks regarding the decision of staying or migrating, $\{\varepsilon^s, \varepsilon^e\}$ distributed according to an Extreme Value Type-1 (Gumbel) with scale parameter κ, that enter additively to their value functions. These shocks make the migration decision probabilistic from an ex-ante perspective and allow agents to migrate for non-economic reasons.

Living in the U.S. Once the agent arrives in the U.S., every period receives the utility mentioned above. Still, it is subject to an exogenous deportation probability of $\psi \in [0, 1)$, representing the risk of being caught by immigration authorities in the U.S. In this case, the agent is sent back to the home economy. While with probability $(1 - \psi)$, the agent continues to reside in the U.S. for another period. The sum of agents abroad and at home must equal the continuum of agents.

Climate Change. Over time, the mean of the temperature distribution increases. This affects the distribution of high-heat shocks, making them worse and more frequent year after year. Agents at home can foresee this and make decisions accordingly. We assume climate change has no effect on the consumption levels of migrants in the U.S.

3.2 The Migration Problem

Below, we write the problems in their recursive formulation. An agent with permanent productivity η has two state variables: the agents' level of assets a and the idiosyncratic transitory heat shock z. We start with the migration problem faced by agents in the home economy.

Value at the Home Economy. We denote the ex-ante value function as the expectation over the taste

shocks as $\mathcal{V}_t(a,z,\eta)$. Agents at home solve

$$\mathcal{V}_t(a,z;\eta) = \mathbb{E}_\varepsilon\left[\max\left\{V_t^s(a,z;\eta)+\varepsilon^s, V_t^e(a,z;\eta)+\varepsilon^e\right\}\right] \tag{5}$$

Where agent η chooses between migrating or staying, with $V_t^s(a,z;\eta)$ representing the value of staying, while $V_t^e(a,z;\eta)$ is the value of migrating today. Assuming the taste shocks are iid across agents and options, we obtain the probability of migrating in closed form under distributional assumptions for these shocks.[9] We note that, in general, an increase in the variance of these shocks tends to increase the importance of non-economic reasons leading to migration.

Value of Staying. Conditional on staying, the agent solves the following problem

$$V_t^s(a,z;\eta) = \max_{a'\in\mathcal{A}}\left\{u(wz\eta + a - qa') + \beta\mathbb{E}_t\left[\mathcal{V}_{t+1}(a',z';\eta)\right]\right\} \tag{6}$$

The staying agent only chooses consumption and savings levels. Borrowing is not allowed, meaning $a' \geqslant 0$, or equivalently, 0 is the lowest point in $\mathcal{A}$. Combined with the budget constraint, savings decisions pin down the consumption level, now equal to the wages received by the agent, plus the level of assets at the beginning of the period minus the expenditure on assets for the next period. The second term inside the maximization problem corresponds to the discounted continuation value of being at the home economy. The value depends on the future realization of the transitory high-heat shock, z', and the asset holdings carried forward, a'. In the model, agents will save either to smooth consumption or to migrate eventually.

Value of Migrating. The value of migrating is the following

$$V_t^e(a,z;\eta) = u(wz\eta + a - m^e) + \beta\left[\mathbb{E}_t\left[\phi V_{t+1}^*(\eta) + (1-\phi)\mathcal{V}_{t+1}(0,z';\eta)\right]\right] \tag{7}$$

with $V_t^e(a,z;\eta) = -\infty$ if $wz\eta + a < m^e$. The migrant's problem is passive. First, since the agent cannot take assets abroad, the budget constraint pins down the consumption level. The agent can only migrate if the budget constraint is satisfied and consumption is non-negative, i.e., if it can pay the migration cost. Aside from the taste shock, a necessary condition for the agent to migrate is that the future expected utility

[9] We show further details on Appendix B.

in the U.S. must be higher than the one at home. In this problem, the discounted continuation value has two components. With probability ϕ, the agent successfully migrates, and next period obtains a value of $V^*(\eta)$, which represents the value of living in the U.S. With probability $(1-\phi)$, the agent is detained while trying to migrate and is sent back to the home economy without any assets, $a' = 0$ and will be subject to a high-heat shock z' next period.

Value of Living in the U.S. When the agent is living in the U.S. the value is the following

$$V_t^*(\eta) = u(c^*)\nu + \beta\left\{\mathbb{E}_t\left[(1-\psi)V_{t+1}^*(\eta) + \psi\mathcal{V}_{t+1}(0,z';\eta)\right]\right\} \tag{8}$$

The agent in the U.S. receives a risk-free consumption level every period of c^*; however, the period utility is discounted by ν, which is the disutility of adapting to the U.S.[10]. The discounted expected continuation value of being in the U.S. will be affected by the probability of being sent back home ψ. With probability $(1-\psi)$, the agent stays one more period in the U.S. and obtains $V^*(\eta)$. With probability ψ, the agent is sent back to the home economy without assets and is subject to a high-heat shock the next period. Given the possibility of returning to the home economy, the value of being in the U.S. depends on the permanent productivity level η. The value does not depend on the current heat shock z, since the shocks are iid and do not affect the period utility in the U.S.

Stationary Distribution. If the distribution of high-heat shocks is constant, the model exhibits a stationary distribution of agents. We then can drop the subscript t of the value functions. We use this approach to estimate the model, as we discuss in section 4. Here, we provide a short description of the stationary distribution and refer to Appendix B for further technical details.

In the model, there is a unitary mass of agents. This mass is composed by agents living in Guatemala, which we denote as $\mu(a,z,\eta)$ and Guatemalan migrants in the U.S., M. Agents in Guatemala are subject to shocks z and hold asset position a. The migration and savings policy functions, together with the success and deportation probabilities, in addition to the exogenous law of motion of shocks, imply the laws of motion for the stock of agents in Guatemala, $\mu(a,z,\eta)$, and in the U.S., $M(\eta)$. Agents in Guatemala can either stay or migrate, and conditional on staying, they choose a particular asset position a' given their state (a,z,η), and will receive a shock z' next period. Some agents will successfully migrate to the U.S.,

[10] In Appendix H, we provide a comprehensive discussion about this parameter ν.

while others will be detained at the border or deported back to Guatemala. The stationary distribution is a pair (μ, M) such that these flows remain constants across the state space (a, z, η).

3.3 Comparison to the Workhorse Model

Before proceeding to the estimation, we compare our model to Caliendo et al. (2019), the workhorse quantitative dynamic migration model in the literature. Here, we explain the economic intuition of why the reference model is not well-suited to explain the high-heat migration link, β_e, from Table 1. We refer to Appendix B for further details.

The data shows a tight link between current temperature and following-period migration across space. Our mechanism relies on crop yields: good weather conditions translate into generous income and allow agents to pay the migration cost. In general, with poor agents, the consumption level conditional on staying is higher than the one conditional on migrating, leading to a higher valuation of extra income for the migrant than for the stayer. Thus, when the weather conditions dry up, and income falls, the value of emigrating falls more than the value of staying. As a result, in general, the migration probability decreases under a low realization of z, holding a and η fixed.

In comparing the evidence with the workhorse model in the dynamic migration literature, Caliendo et al. (2019), we modify our model in several dimensions to make it resemble the main ingredients of them. In such a version, agents are subject to the same temporary shocks z, but do not have any asset available to save, $a = a' = 0$, and the monetary migration cost m^e is null. Instead, as in Caliendo et al. (2019), agents face a disutility of migration in terms of utility, $\tau \geqslant 0$, which is independent of z.

The parameter τ clearly can make migrating more or less attractive relative to staying, and hence, is useful to estimate the mass of agents in the U.S., M, as we do in Section 4 for our baseline model. A higher value of τ tends to decrease this mass M monotonically. This τ, however, cannot make it the cross-sectional evidence in Table 1, since it does not distort the relative valuation of consumption under different z shock realizations conditional on migrating relative to staying, as we have in our model.

In Appendix B, we illustrate exactly this point by showing how this additive utility cost of migrating is completely unrelated to the *marginal* effect of high-heat on migration. As we show there, the parameter can, in fact, be used to match perfectly the mass of migrants in the U.S. Hence, focusing on *just* the share

is *not enough* to pin down what is exactly behind the migration decisions.

4 Model Solution and Estimation

In this section, we describe our estimation strategy, the model's solution in a stationary equilibrium and the negative link between high heat and migration produced by the model, and climate change projections.

First, we start by assigning values to specific parameters that are either directly observed in the data, standard in the literature, or estimated externally. Second, we use indirect inference to jointly estimate the monetary migration cost, m^e, and the disutility of living abroad, ν; these parameters are key to our negative heat-migration link and the stock of Guatemalan migrants in the US. For estimation purposes, we assume the economy is initially at a stationary distribution; this is equivalent to a no-climate-change scenario. Third, we discuss the model's migration and savings decisions and how they produce the negative high-heat migration link. Finally, we obtain temperature projections for each climate change scenario in the region of Guatemala; then, we derive the trajectories of high-heat shock distributions and compute the paths for rural yields. In the next subsection, we proceed to describe the externally calibrated parameters.

4.1 Externally Calibrated Parameters

We begin by setting parameters to values that can be directly observed in the data or obtained from the existing quantitative macroeconomic literature. Table 2 summarizes the externally calibrated parameters. We choose the time period to be a year. We set the coefficient of relative risk aversion σ to be 2, and the discount factor β to 0.95. These are standard values in the macroeconomics literature for the annual frequency. Additionally, we set the taste shock scale parameter, κ, to 0.478, as found in Bilal and Rossi-Hansberg (2023).

We then determine the gross rate of return on savings, q^{-1}, as the average difference, for the 2011-18 period, between the interest rate of deposits in Guatemala, and the inflation rate (World Bank, 2023); the result is a 1.27% annual real interest rate. We obtain the success probability of Guatemalan migrants arriving in the U.S., ϕ, from Carare et al. (2023); this is equal to 0.50. We calculate the deportation

Table 2: Externally calibrated parameters

Parameter	Value	Explanation	Reference
σ	2.00	CRRA coefficient	Standard
β	0.95	Discount factor	Standard
κ	0.478	Scale of taste shocks ϵ^e, ϵ^s	Bilal and Rossi-Hansberg (2023)
q	$(1.0127)^{-1}$	Inverse of rate of return of asset	Deposits - Inflation rate
ϕ	0.50	Success probability	Carare et al. (2023)
ψ	3.29%	Deportation probability	Removals/Unauthorized Population
c^*	$4.29 \times \mathbb{E}[z]$	Consumption level in the U.S.	U.S.-Guatemala wage ratio, PPP adjusted
μ_η	0.00	Mean of $\log(\eta)$	Normalization
σ_η	0.71	Standard deviation of $\log(\eta)$	$\mathbb{SD}[\log(\eta)\|\text{stay}] = 0.71$
α	1.00	Production return to scale	Constant Return to Scale
χ	2.30%	High-heat yield drop	See Section 4.2

probability, ψ, as the ratio of average annual removals for 2011-18 (US DHS, 2022), divided by the total undocumented population in the U.S. for 2019 (MPI, 2023); thus, we set the probability to 0.0329. The consumption level for Guatemalan migrants in the U.S., c^*, is calculated as the average annual personal income of Guatemalans in the U.S. for 2016 (Ruggles et al., 2023), divided by the average annual personal income in Guatemala (INE, 2016), both values are in PPP for the year 2016 (IMF, 2023); the resulting ratio is 4.29. We then multiply it by the average realization of the high-heat shock on rural productivity under the average η.

We normalize the mean of the distribution for the agent's time-invariant productivity, μ_η, to 0. To determine the standard deviation of the distribution, σ_η, we use the latest agricultural census data and estimate the standard deviation of observed yields among farmers. This results in 0.71; thus, we set σ_η to that value. An in-depth explanation of the methodology employed in constructing the farmers' yields is available in Section D.1 of the Appendix.

We set the parameter controlling the returns to scale in the production function, α, to 1. A direct implication is that the wage rate remains unaffected by variations in the amount of efficient labor units in the home economy. Hence, the wage level, w_t, is equal to 1 for every period. Finally, the yield drop induced by one complete day of exposure to temperatures above 30°C, χ, is set to 2.3%. The next subsection provides further details on this.

4.2 Link between High-Heat Shocks and Rural Productivity

Since rural productivity data from Guatemala is not readily available, we compute the productivity drop from one day of exposure using the dataset from Schlenker and Roberts (2009), which uses U.S. data. We opt to use the estimate for corn, given its predominance in Guatemala's agriculture, occupying 36.6% of croplands as indicated in (FAO, 2023; INE, 2020). We run a Fixed-effect specification with log corn yields against exposure and several other control variables. Further details about the specification and the results can be found in Section A.2 of the Appendix. The estimated effect of exposure on log yields is -0.023, meaning an increase in one exposure day decreases corn production by 2.3%. Therefore, we set our χ to be 0.023. Subsequently, we compute the distribution for z, combining our estimated χ and the exposure distribution for Guatemala. Further details can be found in Section C.3 of the Appendix.

4.3 Simulated Method of Moments

We estimate the two remaining parameters using Simulated Method of Moments (SMM). In this approach, we choose the parameter vector that minimizes the distance between the moments in the data and the simulated ones in the model. This distance is represented by a loss function. In Section E of the Appendix, we highlight the more salient details on the computational implementation of the SMM.

The parameters we estimate are the monetary migration cost, m^e, and the disutility of being abroad, ν. We then choose two data moments to match, for which our parameters are informative. The first targeted moment is the coefficient of the high-heat migration link we report in Table 1. The second moment is the share of undocumented Guatemalans in the U.S., which is equal to 7.4%.[11]

Computation of Model's Moments. The model generates two moments for comparison with their empirical counterparts. The first, β_e, is the analog regression coefficient to that found in Table 1 and is subject to sampling variation. The second, the stock of migrants in the U.S., M, emerges from the model's stationary distribution. To evaluate the distance between data and model, we start by choosing a tentative parameter vector. We solve the policy functions and find the stationary distribution; here, we compute the model's simulated stock of migrants, M. We then randomly sample agents in the model from the stationary distribution and estimate the model's β_e. The sampling procedure is simulated a thousand

[11] In Section I of the Appendix, we show how the parameters identify the moments and other robustness exercises.

times to calculate the model's average coefficient, $\hat{\beta}_e$, across samples. Finally, the distance between the moments is evaluated, and a new parameter vector is chosen. This process is done iteratively until the distance between data and model moments is close enough.

Estimation Results. Below, we report and discuss the estimated parameters. Table 3 shows the actual data moments, the corresponding moments generated by the model, and the values of the estimated parameters. The model does a good job of delivering the targeted moments. The estimated model slightly overestimates the impact of the high-heat shocks on migration and the share of migrants in the U.S.

Table 3: Targeted Moments and Parameter Results

Moments	**Data**	**Model**
Migration drop induced by exposure, β_e	-0.880	-0.882
Migrant share of Guatemalans in the U.S., M	0.074	0.076

Parameter	**Value**
Migration cost, m^e	2.47
Disutility of living in the U.S., ν	2.58

Note: This table shows the actual data moments, the moments generated by the model, and the values of the estimated parameters. Please note that the disutility of living in the U.S., ν, is positive, consistent with a CRRA utility function where σ equals 2, implying negative utility function values. $\nu > 1$ represents a lower utility of living abroad, while $0 < \nu < 1$ does the opposite.

It is straightforward to see that both parameters, $\{m^e, \nu\}$, are tightly related to the stock of Migrants M. A higher migration cost, m^e, lowers the period utility of the potential migrant, making migration less attractive. A higher disutility of living abroad, ν, decreases the utility in the U.S., decreasing migration incentives. Ultimately, this leads to a lower stock of Migrants in the U.S., meaning an increase in the value of any of both parameters decreases M.

However, the migration cost, m^e, is more closely related to the sensitivity of the migration rates to the high-heat shocks, β_e than the disutility of living abroad. This important difference arises from the impact of m^e on the relative valuation of an extra amount of income, which translates partially or fully into consumption under the path of staying or migrating. This stark economic intuition lies in the deep core of our model.

Model Fit. Given the simplicity of the model and the lack of availability of granular data from

Guatemala, it is difficult to run external validity exercises. Using data from the "Survey on International Migration of Guatemalan Persons and Remittances 2016", we estimate the average migration cost of hiring a smuggler in proportion to the average wage in Guatemala (INE, 2016), this results in 1.92 for the year 2016. In the context of the model, it is approximated to be $1.92 \times \mathbb{E}[z]$, under $\eta = 1.0$. The estimated parameter m^e is 2.47 and, hence, is slightly higher than the equivalent of the data counterpart. This result should not be surprising, as a higher m^e cost detains migration — it is, in fact, capturing other forces that disincentive migration that we do not model explicitly.

Additionally, we set σ_η so that the standard deviation of $\log(\eta)$ conditional on staying is approximately 0.71. We take this route because we can observe, in the data, only individuals who stayed in Guatemala. This moment in the model is clearly endogenous: it depends on the self-selection of heterogeneous agents that decide to stay. The result after the estimation is 0.72.

4.4 Migration and Savings Decisions

In this section, we present the model's migration probabilities and savings decisions. First, we show how the migration decision depends on the high-heat shock, the level of assets, and the agent's productivity. Second, we discuss the savings policy functions for the same agents under two high-heat shocks and how they relate to migration decisions.

Figure 2 depicts the migration probability across different asset levels and high-heat shocks for two distinct agent types. The left panel represents an agent with productivity below the median, while the right panel shows one above the median. The vertical axis represents the magnitude of the high-heat shock, whereas the horizontal axis indicates the agent's asset level. The color pallet in the vertical-right-axis represents the probability of migrating. A darker color means a higher probability of migrating, while lighter hues imply a lower probability.

For both types, a high-heat shock that decreases rural productivity z also decreases the probability of migrating in regions of the heatmap where the asset level is close to the migration cost. An agent with assets approximating the migration cost can pay the cost under a positive shock. However, migration is either unfeasible or very costly in terms of period utility under an unfavorable shock. This result aligns with the data moment we match β_e: negative shocks decrease migration rates. The moment sheds light on

Figure 2: Probability of Migration for low and high productivity agents

(a) Migration Probability for low-productivity type

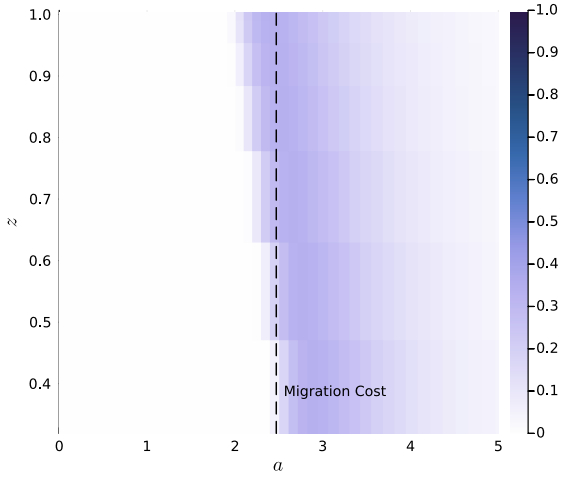

(b) Migration Probability high-productivity type

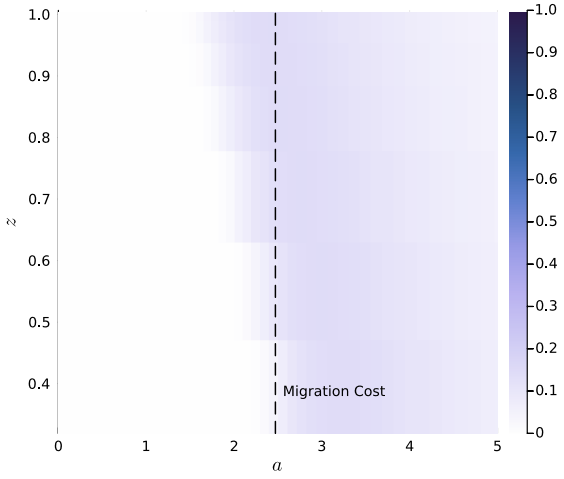

Note: Panel (a) shows the migration probability for an agent with permanent productivity η equals to 0.8. The vertical axis is the realization of the high-heat shock, z, and the horizontal axis shows the current asset holdings a. Panel (b) shows the same migration policy function, but for η equals to 1.3.

Figure 3: Savings Decisions for low and high productivity agents by high-heat shocks

(a) Savings decisions for low-productivity type

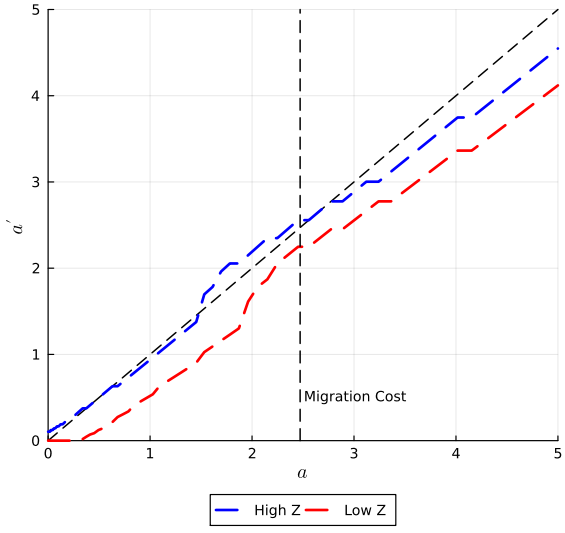

(b) Savings decisions for high-productivity type

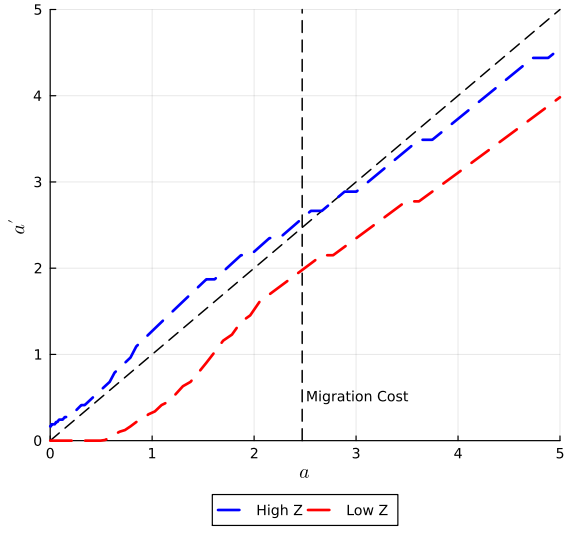

Note: Panel (a) shows the asset holdings chosen for the next period by an agent with permanent productivity η equals to 0.8. The vertical axis is the next-period asset holdings, a', and the horizontal axis shows the current asset holdings a. The blue curve represents the best shock ($z = 1$, no heat), and the red shows the worst ($z = 0.39$). Panel (b) shows the same savings policy function, but for η equals to 1.3.

the fluctuating migration probabilities for agents with credit constraints under different high-heat shocks.

For regions in the heatmap close to the migration cost, the probability of migration is more intense for the low-productivity agent compared to the high-productivity.[12] This partially comes from the fact that the agent with lower productivity has a lower expected income flow at home compared to the high-productivity agent. Additionally, the high-productivity agent does not benefit from such productivity upon migrating to the U.S.

Lastly, agents with more assets tend to have lower migration probabilities. This is especially pronounced for agents with low productivity. In this case, agents prefer consuming their assets before migrating, given their inability to transport them to the U.S.

Even though migration probabilities might suggest higher migration flows coming from low-productivity agents, we need to analyze the savings' policy functions. In Figure 3, we plot the savings policy functions for the same agents from Figure 2. Here, the blue line indicates the policy function under a good productivity shock (absence of high heat), while the red illustrates the function for the worst high-heat shock. The horizontal axis represents the current agent's asset level, while the vertical axis represents the agent's asset level for the next period, a'.

First, we see that both agents accumulate assets during good times up to some asset thresholds. In our model, there are two main reasons why agents save. The first one is the most intuitive: upon receiving good shocks and by the concavity of the utility function, the agent is better off by consuming some extra income today and saving some of it for the next period, insuring against a bad shock. Notice when agents receive an unfavorable high-heat shock, they consume part of their assets to smooth consumption, effectively dis-saving.

The second reason why agents save is to pay the migration cost. For example, looking at the low-productivity agent in Figure 3a, under a good shock, if her assets holdings are between 1.5 and m^e, she would accumulate assets. The observed jump at approximately $a = 1.5$ points towards agents starting to save to pay the migration cost and migrate potentially upon receiving a sequence of favorable shocks.[13]

[12] For even lower-productivity agents, the migration cost is equivalent to several years of income. Considering the chance of being detained at the border and losing all their assets, it is optimal for such agents not to migrate, even if they can afford to migrate.

[13] Figure 2a shows at this asset level and under this shock, the probability of migration is zero: the agent will have to save for migrating later, eventually, upon facing a sequence of good shocks.

However, in the stationary state, the low-productivity agent does not migrate. Assuming the agent can afford the migration cost, eventually, it returns home with zero assets.[14] Once back in the home economy, the agent accumulates assets under positive shocks up to approximately $a = 0.5$. Beyond this point, the agent ceases to accumulate. Considering that the probability of migration is zero at this asset level, this agent will not migrate in the stationary state.

Analyzing the high-productivity agent, we see positive migration flows in the stationary state. Under a sequence of good shocks, the agent will accumulate assets, eventually reaching an asset level that puts her in a region of the heatmap, Figure 2b, where she is willing to pay the migration cost, increasing the migration probability.

The dynamics exposed in this section show that the link between high heat and migration does not depend on the agent's productivity type. For both low and high types, the migration probability decreases when the agent suffers a high-heat shock. In the stationary state, we do not see migration flows coming from the low type, but we do from the high type. Given that higher types generate more income, they are less constrained to migrate; however, the reduction in current consumption associated with paying the migration cost and a high-heat shock makes it very costly to migrate in terms of period utility.

4.5 Climate Change Projections

Once the model is estimated, we obtain temperature projections for different climate change scenarios from the Intergovernmental Panel on Climate Change (IPCC) (Gutiérrez et al., 2021). These projections are specific to the Central American region during the main crop season from April to September. We consider three climate change scenarios: optimistic, moderate, and pessimistic.[15]

In Figure A.6 of the Appendix, we plot the projected temperature increases across the distinct scenarios relative to the 1995-2014 period and their quadratic fit.[16] There are three scenarios. The optimistic scenario indicates temperatures will peak around 2050 and gradually decline, reaching a final

[14] Every period, there is a share of migrants being detained at the border or deported. Recall that upon trying to migrate, agents face a success probability equal to $\phi < 1$. Additionally, every period upon being in the U.S., there is a probability of facing deportation, $\psi > 0$. Thus, upon trying to migrate, every agent eventually returns to Guatemala, either from being detained at the border or from deportation procedures.

[15] The scenarios correspond to the scenarios defined by the IPCC as RCP2.6 (optimistic), RCP4.5 (moderate), and RCP8.5 (pessimistic). We collect the projection numbers in July 2023.

[16] A quadratic fit offers a good balance between simplicity and goodness of fit. In particular, for the optimistic scenario, but also for the moderate one, temperatures rise up to a point and then decrease. A linear fit seems, therefore, inappropriate.

increase in temperature of 0.7°C by 2100. The moderate scenario anticipates a temperature increase of 1.6°C by 2100. The pessimistic scenario forecasts an increase of 3.3°C. In our analysis, we assume that temperatures stop changing by 2100.

Using these projections, we compute a distribution for Z for every projected year and scenario. Details about the construction of the Z distribution for every year of the transition can be found in Section F of the Appendix.[17] Figure 4, plots the projected average productivity path relative to the initial average for the three scenarios. In the optimistic scenario, the drop in average productivity is around 3% by 2070, slightly recovering at the end of the period as temperatures start to cool down. In the moderate scenario, the drop resembles to be linear, dropping 10% in average productivity at the end of the period. The drop is more accelerated and pronounced for the pessimistic scenario, with average productivity plummeting by around 25% by 2100.

Figure 4: Average Productivity Relative to Baseline by Scenario

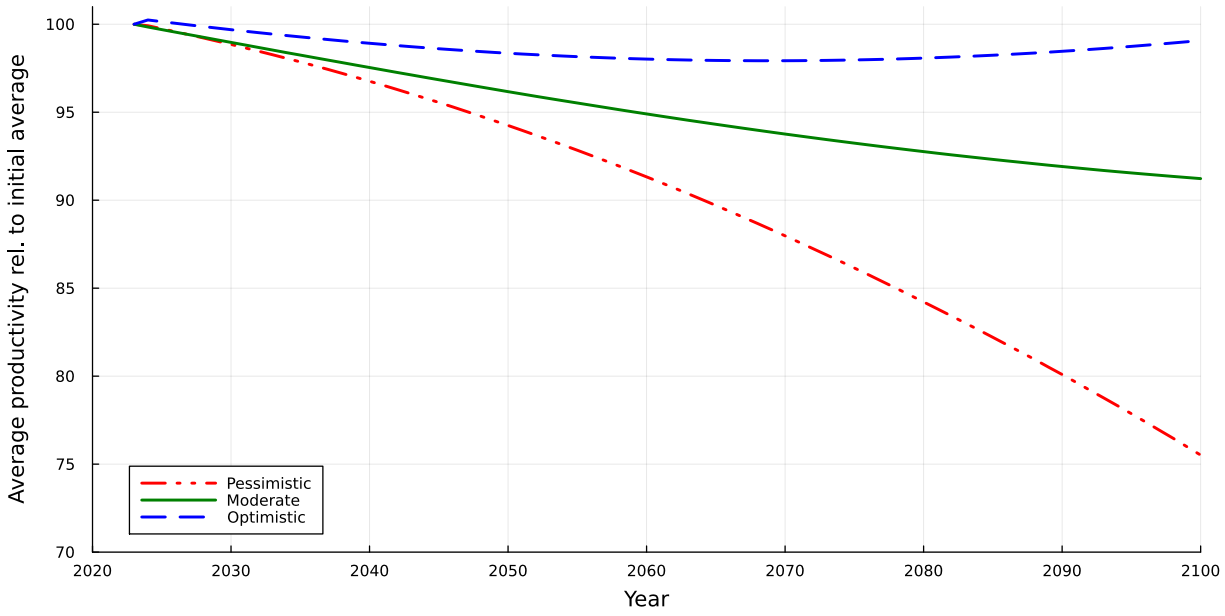

Having projected the entire distribution of productivity shocks for every scenario over the projecting years, we feed these sequences into the model. For our main results, we designate 2023 as the year in which agents become aware of climate change and can foresee changes in productivity. In our analysis, there is no uncertainty about the climate change scenario agents will experience. Agents know the entire

[17] Additionally, in Figure A.7 of the Appendix, we plot the initial distribution of exposure and the final distribution for every scenario in the year 2100, the last year of the transition.

path for the distribution of productivity, and they make decisions accordingly. Agents are still subject to idiosyncratic shocks throughout the transition path, but the current and future distributions are perfectly foreseeable to the individuals.

5 The Effects of Climate Change

In this section, we present a series of results and counterfactuals to analyze different scenarios. First, we present the main results from our model. Second, we isolate the effects of anticipation, comparing our main results to a scenario where agents take the current transitory productivity distribution as permanent sequentially. The key results are intuitive: as soon as agents are aware of climate change, migration flows increase; additionally, anticipation effects are strong, agents with perfect foresight exhibit higher migration flows in the short and medium run than agents who cannot anticipate climate change. Next, we present our main results.

5.1 Main Results

We start with an economy in the stationary state with agents distributed according to their ergodic distribution. In 2023, agents become aware of climate change and learn the entire transitional path of productivity distribution.

Figure 5 displays the annual migration flows of Guatemalans migrating to the U.S. The y-axis represents the percentage of the Guatemalan population that has chosen to migrate.[18] Looking at the figure, we see migration flows increasing under all scenarios. The increment is most pronounced in the pessimistic scenario and least in the optimistic one. Relative to initial migration, by 2040, migration flows increase by 106%, 71%, and 35% in the pessimistic, moderate, and optimistic scenarios, respectively, marking the peak for the moderate and optimistic scenarios. In the pessimistic case, by 2070, the increase in migration flows relative to the initial period is 179%, reaching its peak. Ultimately, migration flows reach a stationary level. By 2100, the stock of Guatemalan migrants in the U.S. rises by 138%, 63%, and

[18] Percentages are over the total Guatemalan population located in Guatemala and the U.S. Also, it is important to distinguish between the decision to migrate and successfully arriving in the U.S. Agents succeed in migrating at a rate of ϕ.

17% for the pessimistic, moderate, and optimistic scenarios, respectively.[19]

Figure 5: Effect of Climate Change on Migration Flows

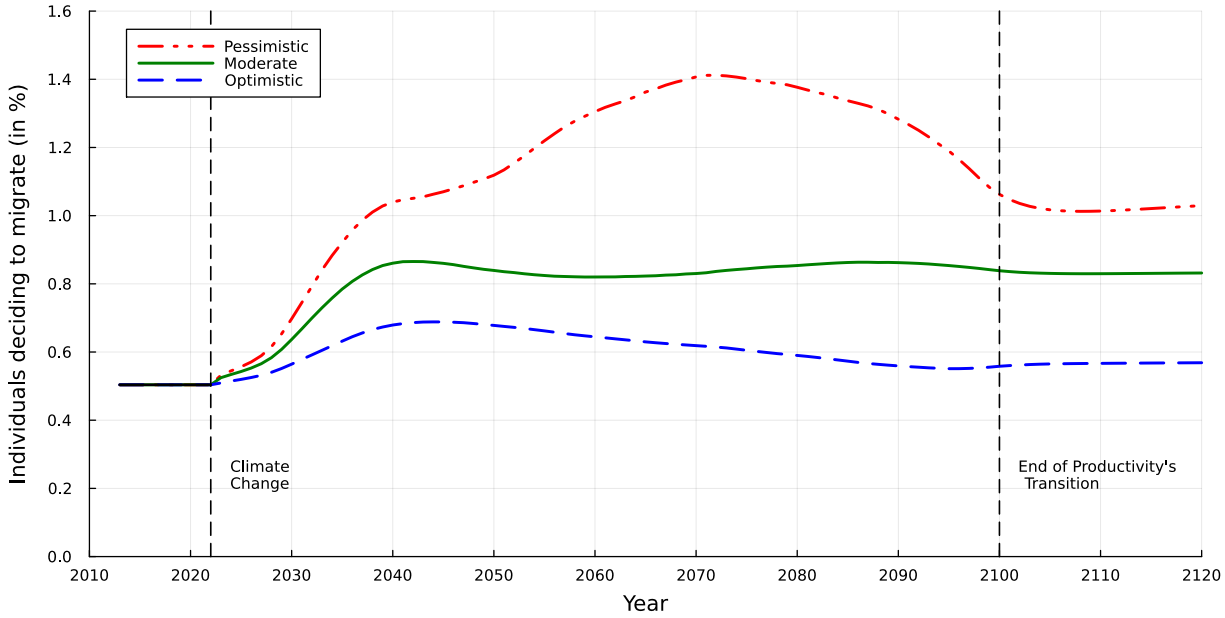

Note: The vertical axis represents the percentage of the Guatemalan population that decides to migrate. It is important to distinguish between the decision to migrate and successfully arriving in the U.S. Agents succeed in migrating at a rate of ϕ. Furthermore, the percentages are over the total Guatemalan population located in Guatemala and the U.S.

Under climate change, agents anticipate a reduction in future income in Guatemala, increasing migration's appeal. This happens for all agents under all scenarios. Figure A.10 of the Appendix highlights this pattern, where we can see how the stock of migrants in the final stationary state increases for all productivity types compared to our initial state.

Diving a bit more into the dynamics, the increase in migration flows is smooth and gradual. The smoothness is attributed to the large mass of low-productivity agents willing to migrate but initially constrained by insufficient assets. These individuals must build up savings over time until they reach a level of assets that allows them to pay the migration cost. The lower the agent's productivity, the longer it takes to save enough to afford the migration cost. Specifically, in the pessimistic case, the fall in income is so strong that, close to the year 2050, a new lower productivity agent starts saving for migration, explaining the acceleration in the migration flows for the subsequent periods.

Additionally, in the pessimistic scenario,[20] the stock of migrants overshoots (Figure A.8 of the

[19]The evolution of the stock of migrants can be found in Figure A.8 of the Appendix.

[20]Looking at the optimistic scenario, there seems to be overshooting; however, a big part of this is because, in this scenario, things get better after the year 2070. This is shown in Figure 4.

Appendix). The overshooting is a byproduct of the combination of anticipation and future conditions. Agents not only anticipate things will get worse trying to migrate early but also know it will be harder to migrate later as income decreases. This leads to some agents migrating during the transition but not in the final stationary state, as during the transition, when things are not as bad, it is easier for them to save up and pay the migration cost. After peaking,[21] the stock starts decreasing. Before the end of the productivity transition, income is so low that migration becomes too costly.

Even though the high-heat migration link, β_e, might suggest that under climate change, more people would be constrained and unable to migrate, our main results indicate the opposite. However, how is this result consistent with the heat-migration link? We proceed to answer this question by analyzing Figure 6. This graph plots the model's estimated heat-migration link for every year and scenario. The vertical axis represents the regression coefficient $\hat{\beta}_e$ for each point in time. The followed procedure to compute $\hat{\beta}_e$ is the same we used to compute the coefficient for the SMM estimation.[22]

Figure 6: Effect of Climate Change on the High-Heat Migration link (β_e)

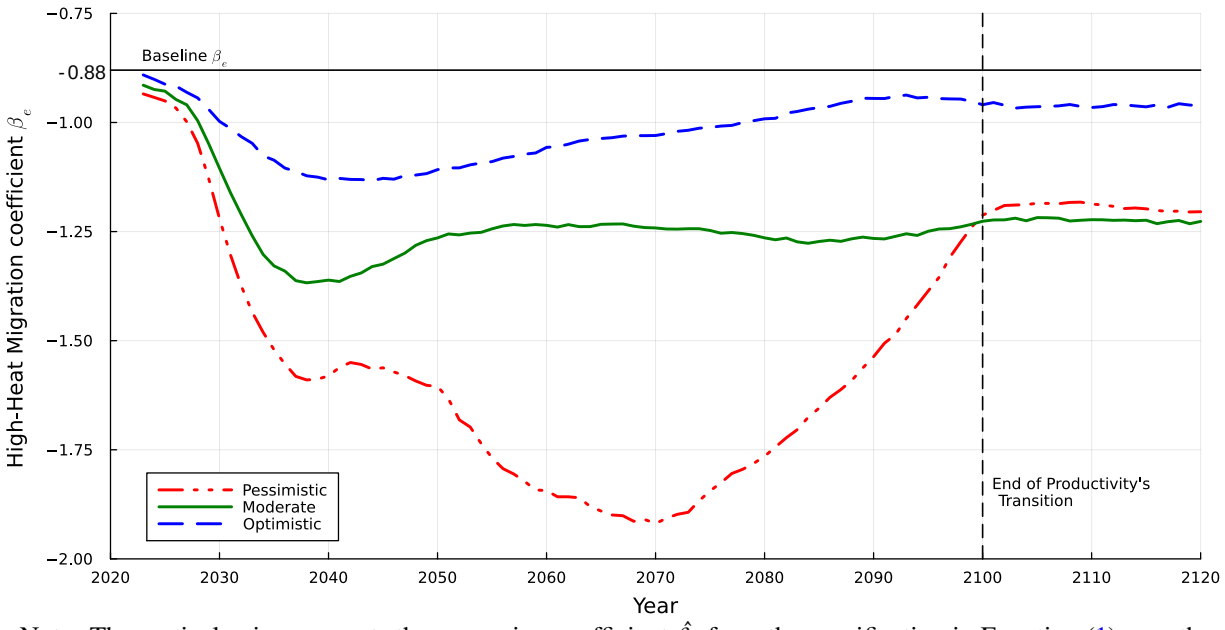

Note: The vertical axis represents the regression coefficient $\hat{\beta}_e$ from the specification in Equation (1) over the transition for different climate change scenarios. The solid black line shows the regression coefficient reported in Table 1. For each point in time, the plotted series follow the same computational procedure of $\hat{\beta}_e$ described in Section 4.3. At each point in time, we collect 1,000 samples with a size of 10,000 individuals. We run a regression for each sample, record the estimated β_e coefficient, and compute the average across samples, $\hat{\beta}_e$. The plot shows this average at every point in the figure.

[21] A decrease in the stock of migrants implies a negative net migration. This happens as more people are being deported than the ones that are migrating, as migration is getting increasingly costly.

[22] This is described in Section 4.3.

As we can see in Figure 6, the high-heat migration link is consistently negative for all periods and scenarios, meaning our main results are consistent with the link. We see major fluctuations in magnitude across the transition, with the highest for the pessimistic scenario and the least for the optimistic.

5.2 The Role of Anticipation

To account for how much of the migration is attributable to agents anticipating the effects of climate change, we perform an exercise analogous to Bilal and Rossi-Hansberg (2023). In this counterfactual, agents do not foresee future changes in the productivity distribution. They can only observe past and today's heat shock distributions. In the climate change transition, they observe a new high-heat productivity distribution and update their expectations according to that distribution. This allows us to isolate the migration due to agents anticipating climate change.

Figure 7: Effect of Anticipation on Migration Flows by Scenario

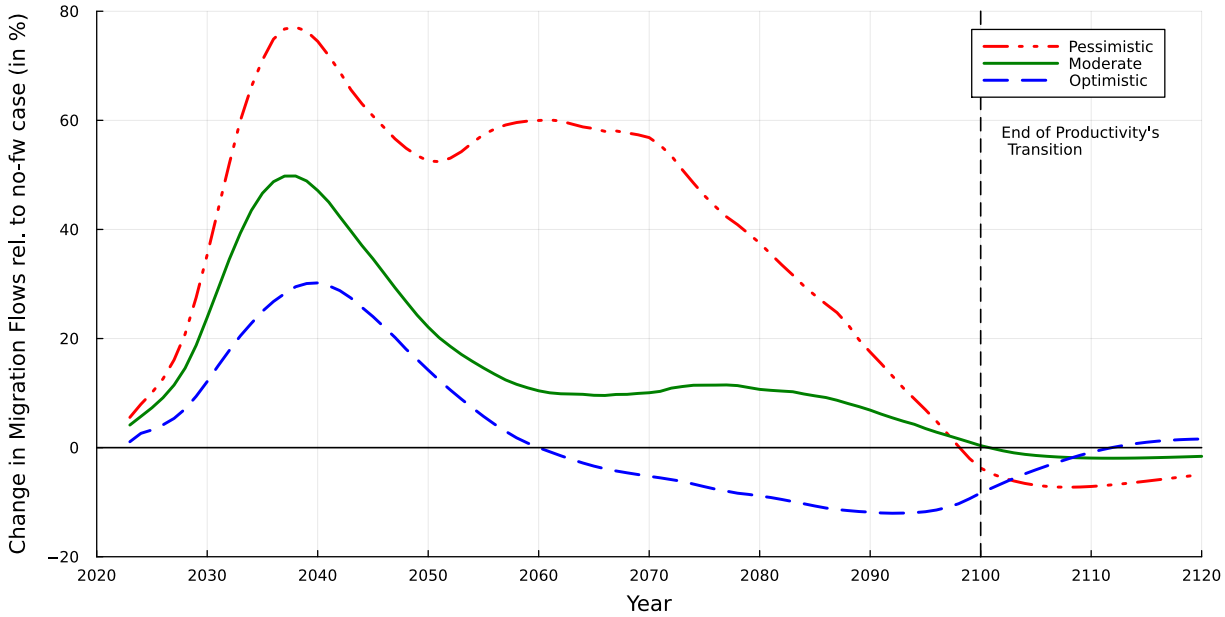

Note: The vertical represents the difference between the agents that migrated in our baseline model and the no-anticipation case, normalized by the latter. Differences are expressed in percentages.

Figure 7 shows the percentage differential in migration flows relative to the no-anticipation case. We see that when agents can anticipate the effects of climate change, migration flows are substantially higher than the no-anticipation case in both the short and medium-run across all scenarios. As agents anticipate the drop in productivity caused by climate change, they seek to migrate in the earlier periods. Before 2040, migration flows in our baseline exceeded those in the no-anticipation case by 77%, 50%, and 30%

for the pessimistic, moderate, and optimistic scenarios, respectively. After those peaks, the differential in flows starts decreasing, ultimately turning negative. In the long run, the stock of agents migrating with or without anticipation must be the same.

The impact on the stock of migrants is further illustrated in Figure A.9 of the Appendix. In the year 2075, the stock of Guatemalan migrants in the U.S. surpasses that of the no-anticipation case by 49%, 15%, and 4% for the pessimistic, moderate, and optimistic scenarios, respectively.

6 Unconditional Cash Transfers and Migration

We now analyze the effects of unconditional cash transfers (UCTs) on migration under climate change. For this exercise, we assume transfers are given to the agents over their lifetime as long as they stay in Guatemala. Agents believe they will obtain the same transfer for the next periods. Furthermore, we assume the transfer is funded through foreign aid. We study two different eligibility schemes. The first scheme is a universal cash transfer given to all agents in the home economy independent from types or shocks. The second scheme targets agents that suffered an extreme high-heat shock, defined as a drop in productivity of at least 40%. The transfer is not proportional to the innate productivity η and appears additive to the budget constraint in Equations (6) and (7).

6.1 Universal Cash Transfer

In the first transfer scheme, all agents in Guatemala receive a transfer equivalent to 10% of the 2023 average income. We assume agents were not expecting the transfer. They start receiving them in the first period they learn about climate change.

Figure 8 shows the effect of the universal transfer on migration flows over different climate change scenarios. In the early periods of the transition, migration flows under the universal UCT are approximately 10% lower than the baseline. This is explained by high-productivity agents deciding to stay instead of migrating, as the cash transfers increase their value of staying relative to their value of migrating. At some point, the negative difference shrinks, driven by an acceleration in the migration flows from low-productivity agents helped by the transfer. From there, we see different effects for different scenarios. In

Figure 8: Effect of a Universal UCT on Migration Flows

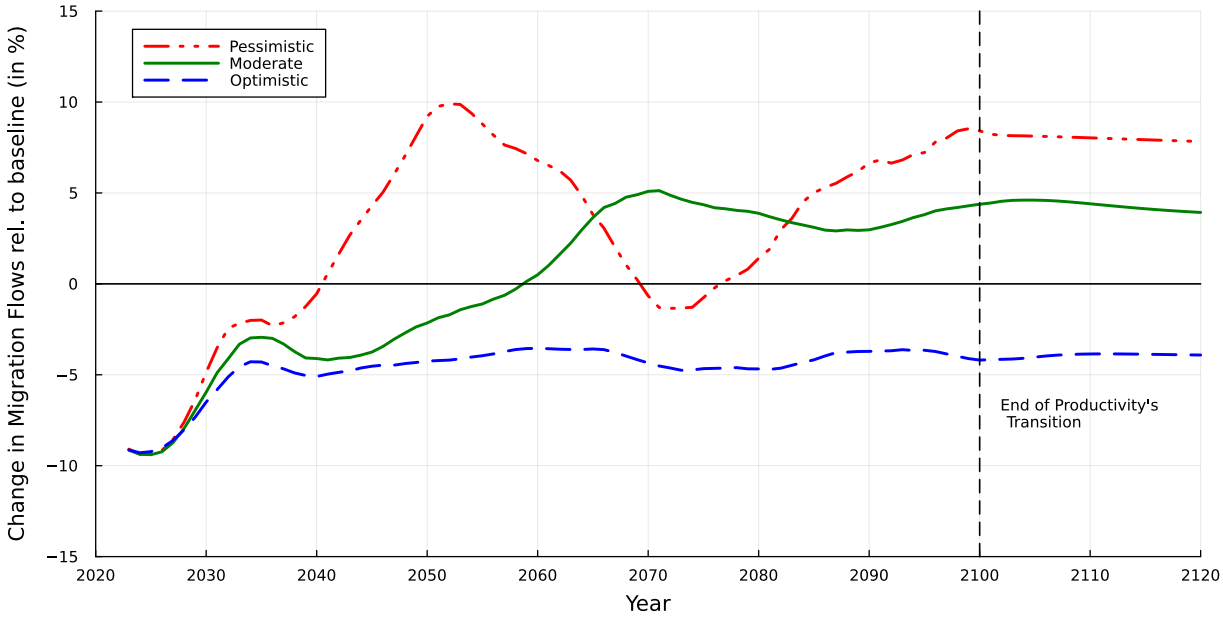

Note: On the vertical axis, we plot the difference between the migration flows under the transfer and our baseline in Section 5.1, dividing it by the baseline. The policy considered here is the Universal UCT, in which every agent receives a cash transfer. The cash transfer is equivalent to 10% of the initial average income.

the pessimistic scenario, the negative difference quickly becomes positive as the transfers keep easing the credit constraints for the low-productivity agents, accelerating the migration process. Subsequently, the difference reaches a maximum and starts ceasing down. This is explained by the time it takes the low-productivity agent to save in order to migrate, an aspect that the transfer accelerates. In the long run, under the new stationary distribution of high-heat shocks, the flow and stock of migrants will be higher with the universal UCT. This also holds for the moderate but not for the optimistic, where the flow is consistently lower.

The transfer shifts the composition of migrating agent types. In all scenarios, transfers shift migration from high-productivity agents to lower ones.[23] The transfer increases income flows every period, making staying more appealing. However, the value of migrating increases as well, given the transfer helps to afford the migration cost. For high-productivity agents, the increase in transfers has a higher effect on the valuation of staying. Before the transfer, their income flow in Guatemala was already high, and in case they needed to migrate, with relatively low savings, they could afford the migration cost; this makes the

[23] In Figure A.12 of the Appendix, we plot the Stock of migrants by type at the final stationary state under both transfers. The shift is observed on the plots located to the left. Although not plotted because of the large amount of periods and types, the same shift is observed during the transition to the stationary state.

effect of the transfer over the value of migrating relatively small. For low-productivity agents, the transfers have a higher impact on the value of migrating. The transfer eases the financial constraint, making it easier to save towards paying the migration cost without sacrificing large consumption levels every period.

6.2 High-Heat Cash Transfer

In this transfer scheme, every agent that receives a bad realization of the high-heat shock receives a transfer. To ease comparisons, we attribute the same transfer amount as in the case of the Universal UCT, 10% of average income. Agents are eligible to receive the transfer if their high-heat shock causes a drop in productivity of at least 40% for that period. The transfer has a relatively small effect on the average income flow agents receive, as the probability of receiving the transfer is 8.4% at the beginning of the transition in 2023. The transfer mainly provides insurance, increasing income under a bad realization of the shock reducing the risk for risk-averse agents. As before, we assume agents were not expecting the transfer, and they received them the first period they knew about climate change.

Figure 9: Effect of a High-Heat UCT on Migration Flows

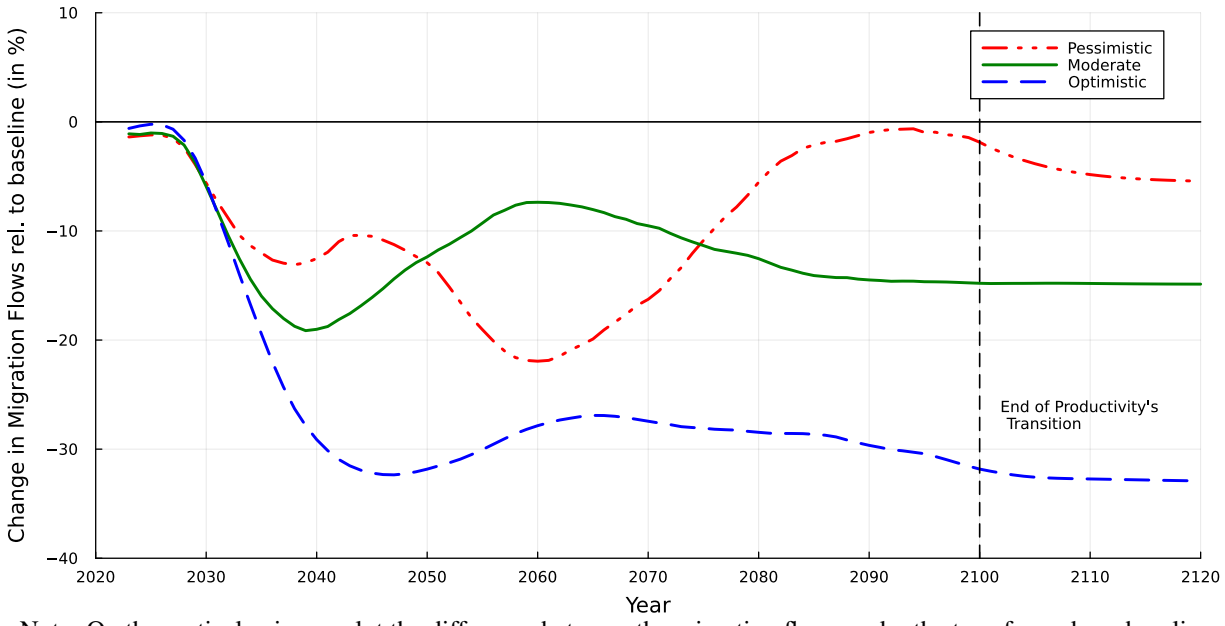

Note: On the vertical axis, we plot the difference between the migration flows under the transfer and our baseline in Section 5.1, dividing it by the baseline. The policy considered here is the High-Heat UCT, in which agents receive a cash transfer in case they suffer a drop in productivity of at least 40%. The cash transfer is equivalent to 10% of the initial average income.

Figure 9 shows the effect of the high-heat cash transfer on migration flows over different climate change scenarios. On the y-axis, we plot the difference between the migration flows under the high-heat

transfer and our baseline in Section 5.1, dividing it by the baseline. Years are plotted on the x-axis.

Examining the dynamics of migration flows, we observe these are consistently below the baseline case for all climate change scenarios. The transfer does not have an immediate effect on the migration trajectories. At the beginning of the period, changes in migration, with respect to the baseline results, are small. After the first few years, transfers start having a larger effect. Migration flows sharply decrease under all scenarios. The effect is more pronounced for the optimistic scenario, where flows under the transfer are 30% lower than those of the baseline results. Under the moderate scenario, migration flows drop up to 20% in 2040, relative to our baseline. After subsequent fluctuations, it eventually converges at approximately 15%. In the pessimistic scenario, migration flows drop up to 22% in 2060, relative to the baseline. Ultimately, the difference shrinks and settles at 5% in the long run.

The decrease in migration flows is generated by the insurance effect of the transfer, especially on the low-productivity migrating agents. The high-heat cash transfer mitigates risk against bad shocks, increasing the agent's value of staying. However, given that the magnitude of the transfer is not dependent on the agent's productivity type, the insurance effect of the transfer is larger for the low-productivity agent compared to the high-productivity.

6.3 Comparing the Transfer Schemes

In our last subsection, we compare two cash transfer schemes, evaluating them concerning migrant stocks and associated costs. Our findings indicate that the high-heat cash transfer not only incentivizes more people to stay in Guatemala but also its cost is significantly lower than a universal cash transfer. We now proceed to compare the stock of migrants under these two transfer schemes.

In Table 4, we show the stock of migrants in our baseline and under the two transfer schemes. We present the stocks for every climate change scenario and different years. The stocks are expressed in percentages of the total Guatemalan population living in Guatemala and in the U.S.

Upon examining Table 4, we can observe that the stock of migrants in the U.S. is lower under the high-heat cash transfer for all climate change scenarios. By 2040, in the medium run, differences with the baseline scenario are 0.7, 0.6, and 0.5 percentage points (p.p.) for the optimistic, moderate, and pessimistic scenarios, respectively. In contrast, the universal cash transfer diminishes migration flows by

Table 4: Stock of Migrants in the U.S. under different Transfer Schemes and Scenarios

Case		2023	2040	2060	2080	2100	2120
Baseline	Optimistic	7.6	8.2	9.2	9.3	8.9	8.8
	Moderate	7.6	8.9	10.8	11.7	12.3	12.5
	Pessimistic	7.6	9.5	13.4	17.1	18.0	16.8
Universal	Optimistic	7.6	8.0	8.8	8.9	8.6	8.4
	Moderate	7.6	8.6	10.5	11.8	12.6	12.9
	Pessimistic	7.6	9.3	13.9	17.5	18.8	17.8
High-Heat	Optimistic	7.6	7.5	6.8	6.2	5.8	5.5
	Moderate	7.6	8.3	9.7	10.6	11.0	10.9
	Pessimistic	7.6	9.0	11.8	15.0	17.1	16.4

Note: This table shows the stock of migrants in the U.S. for the Optimistic, Moderate, and Pessimistic scenarios for our baseline, Universal UCT, and High-Heat UCT. Baseline refers to our main results (no cash transfer). Universal refers to the case in which every agent receives a cash transfer. High-Heat refers to the case in which the cash transfer is received only by agents who suffered a drop in productivity of at least 40%. The cash transfer used for these exercises is equivalent to 10% of the initial average income.

0.2 (optimistic), 0.3 (moderate), and 0.2 p.p. (pessimistic).

In subsequent decades, the disparity between the migrant stocks under the high-heat cash transfer and the baseline becomes increasingly pronounced. By 2080, the difference reaches 3.1 (optimistic), 1.1 (moderate), and 2.1 p.p. (pessimistic). For the same year and under the universal transfer, migrant stocks are similar to the baseline. Notice, for the moderate and pessimistic scenarios, the stocks of migrants are higher than the baseline but lower in the optimistic.

The high-heat cash transfer is more effective in discouraging migration, as it mitigates risk, bolstering the appeal of staying for risk-averse individuals across all climate change scenarios. Conversely, the universal transfer increases cash availability at all times for agents, thereby reducing the financial burden of migration costs and making migration more attractive under most scenarios. We now proceed to a comparative analysis of the costs of each transfer scheme.

In Table 5, we report the cost of unconditional cash transfers (UCTs) and the cost ratio. The first two rows show the annual cost of the universal and the high-heat cash transfers for each climate change scenario, quantified as a percentage of initial average income.[24] The last row shows the cost ratio of the two UCTs, also reported in percentages. As the transfer amount is the same in both schemes, and the only

[24]Initial average income is the average income in Guatemala for 2023.

modification is the eligibility criteria, the high-heat transfer is naturally less costly as it has fewer eligible agents. However, notice that the cost is changing; this is because of two factors. One is the composition of migrants and stayers; the more people stay, the more people will receive the transfer. The second factor only pertains to the high-heat cash transfer; with climate change, the probability of receiving a high-heat shock increases, increasing the number of eligible agents for the transfer.[25]

Table 5: Annual Cost of the Unconditional Cash Transfers

Case		2023	2040	2060	2080	2100	2120
Universal	Optimistic	8.3	8.2	8.2	8.2	8.2	8.2
	Moderate	8.3	8.2	8.0	7.9	7.8	7.8
	Pessimistic	8.3	8.1	7.7	7.4	7.3	7.4
High-Heat	Optimistic	0.7	0.8	1.0	1.0	0.8	0.8
	Moderate	0.7	1.0	1.4	1.7	1.8	1.8
	Pessimistic	0.7	1.1	1.8	2.4	2.9	3.0
$\frac{\text{High-Heat}}{\text{Universal}}$ (%)	Optimistic	8.4	10.2	11.8	11.8	10.0	10.0
	Moderate	8.4	12.4	17.2	21.1	23.0	23.1
	Pessimistic	8.4	13.8	23.0	32.1	40.5	40.4

Note: This table shows the cost of the UCTs for the Optimistic, Moderate, and Pessimistic scenarios. In the first two rows, the cost is annual and measured as a percentage of initial average income. The last row indicates the ratio between the cost of the High-Heat and the Universal cash transfer, expressed in percentages. The cash transfer used for these exercises is equivalent to 10% of the initial average income.

The initial cost associated with a universal transfer equals 8.3% of the average annual income for each agent in Guatemala. In contrast, the high-heat transfer is 0.7%. The ratio between these two schemes is 8.4%, making the high-heat transfer approximately twelve times cheaper than the universal. Notice the cost trajectory of the universal transfer scheme is solely due to changes in the stock of migrants. A decrease in the cost indicates a decline in the Guatemalan population living at home, given the transfer amount is the same across time and agents. In the case of the high-heat transfer, we see a different cost evolution for each scenario. In the optimistic, the cost remains fairly the same, as the drop in productivity generated by climate change is not as severe as in other scenarios, and overall, there is an improvement in weather conditions. In the case of the moderate and pessimistic scenarios, we see a steeper increase in the cost, mainly associated with a higher probability of receiving the high-heat shock. As the cost of the

[25] In Figure A.13 of the Appendix, we show how the probability of receiving such transfer evolves as the productivity becomes less favorable along the transition for each scenario.

high-heat transfer goes up, so does the ratio in the third row. However, notice that the most expensive the high-heat transfer reaches is 40.5% of the universal transfer's cost.

These findings show that not only does the high-heat transfer mitigate risk and make staying more appealing, but it is also significantly less expensive than an alternative where we give a transfer to everyone. However, both exercises come with caveats. Note we assume that the transfer is given throughout the transition, and agents believe that as well. In case agents believe the policy is temporary instead of permanent, results might be different. We could expect transfers to further fuel migration flows, as people are not expecting the policy to last for long. In this case, the institution giving the transfers must have credibility.

7 Conclusion

This paper studies the effects of climate change on international migration flows. Leveraging on census and granular land temperature data for Guatemala, we document a robust negative link between exposure to high heat during the crop season and next year's migration rate to the U.S. We further establish the effect to be stronger in rural areas.

Next, we build a quantitative dynamic migration model in which agents are subject to unfavorable transitory heat shocks that affect their rural yield. At the core of our model high heat decreases income, which ultimately limits agents' ability to migrate. Upon receiving a high-heat shock, the migration cost becomes hard to afford, as sacrificing current consumption has a strong effect on the period's utility, this lowers the agent's migration probability. We show that the mechanism in our model lines up with the feature of our data, something that the standard migration model cannot generate.

We then use the model to study how climate change shapes migration dynamics. There are mainly two major forces affecting migration incentives. On one hand, climate change makes migration more appealing, as rural productivity decreases over time, impoverishing individuals who stay. On the other hand, the worse weather conditions over time reduce available income, making it harder to save and eventually migrate.

We show the effects of two different unconditional cash transfers, funded by foreign aid, on migration flows. In our results, providing a universal cash transfer proves to be both expensive and inefficient. On

one hand, providing cash to some agents makes migration economically viable and triggers migration. On the other, some agents would never migrate regardless of the transfer, and resources are wasted. A scheme that favors insurance against bad shocks decreases migration flows and costs only a fraction of the universal scheme. While we do not provide an explicit objective to be fulfilled with these schemes, the results suggest that there is plenty of room for better targeting and richer schemes.

Our paper abstracts from several mechanisms that can be potentially important for migrating decisions. For example, we do not consider any feedback between agents that stay and factor prices, such as wages or land prices. As more people leave, labor becomes scarce and land abundant. The former tends to make it easier to afford the migration costs, while the latter tends to decrease migration incentives. These simple forces lead to a rich set of possibilities. Furthermore, we assume agents know the scenario they end up experiencing, and they know exactly the entire productivity distribution path. Future work tackling these two assumptions can inform about migrant selection and the role of uncertainty in international migration flows.

References

Adamopoulos, T., Brandt, L., Chen, C., Restuccia, D., and Wei, X. (2022). Land Security and Mobility Frictions. Working Papers tecipa-717, University of Toronto, Department of Economics.

Aiyagari, S. R. (1994). Uninsured idiosyncratic risk and aggregate saving. *The Quarterly Journal of Economics*, 109(3):659–684.

Amirapu, A., Clots-Figueras, I., and Rud, J. P. (2022). Climate change and political participation: Evidence from india.

Bazzi, S. (2017). Wealth heterogeneity and the income elasticity of migration. *American Economic Journal: Applied Economics*, 9(2):219–55.

Bilal, A. and Rossi-Hansberg, E. (2023). Anticipating climate change across the united states. Working Paper 31323, National Bureau of Economic Research.

Buera, F. J., Kaboski, J. P., and Shin, Y. (2020). The Macroeconomics of Microfinance. *The Review of Economic Studies*, 88(1):126–161.

Caliendo, L., Dvorkin, M., and Parro, F. (2019). Trade and labor market dynamics: General equilibrium analysis of the china trade shock. *Econometrica*, 87(3):741–835.

Carare, A., Koh, C., and Yakhshilikov, Y. (2023). Northern triangle undocumented migration to the united states. *IMF Working Papers*, 2023(017):A001.

Cattaneo, C. and Peri, G. (2016). The migration response to increasing temperatures. *Journal of Development Economics*, 122:127–146.

Clement, V., Rigaud, K. K., de Sherbinin, A., Jones, B., Adamo, S., Schewe, J., Sadiq, N., and Shabahat, E. (2021). Groundswell part 2: Acting on internal climate migration. License: CC BY 3.0 IGO.

Copernicus Climate Change Service (2019). ERA5-Land hourly data from 2001 to present.

FAO (2023). Faostat. License: CC BY-NC-SA 3.0 IGO. Accessed on 29 September 2023 at https://www.fao.org/faostat/en/#data.

Gutiérrez, J., Jones, R., Narisma, G., Alves, L., Amjad, M., Gorodetskaya, I., Grose, M., Klutse, N., Krakovska, S., Li, J., Martínez-Castro, D., Mearns, L., Mernild, S., Ngo-Duc, T., van den Hurk, B., and Yoon, J.-H. (2021). *Atlas*. Cambridge University Press. In Press. Interactive Atlas available from http://interactive-atlas.ipcc.ch/.

IMF (2023). World economic outlook database, april 2023. Accessed on 25 August 2023 at https://www.imf.org/en/Publications/WEO/weo-database/2023/April.

INE (2016). Encuesta nacional de empleo e ingresos enei 1-2016. Technical report, Instituto Nacional de Estadística de Guatemala.

INE (2020). Encuesta nacional agropecuaria año agrícola 2019–2020. Technical report, Instituto Nacional de Estadística.

International Food Policy Research Institute (2019). Global Spatially-Disaggregated Crop Production Statistics Data for 2010 Version 2.0.

IOM (2016). Encuesta sobre migración internacional de las personas guatemaltecas y remesas 2016. Tech. rep., International Organization for Migration. United Nations Migration Agency.

Jessoe, K., Manning, D. T., and Taylor, J. E. (2018). Climate Change and Labour Allocation in Rural Mexico: Evidence from Annual Fluctuations in Weather. *Economic Journal*, 128(608):230–261.

Lagakos, D., Mobarak, A. M., and Waugh, M. E. (2023). The welfare effects of encouraging rural–urban migration. *Econometrica*, 91(3):803–837.

Mbow, C., Rosenzweig, C., Barioni, L. G., Benton, T. G., Herrero, M., Krishnapillai, M., Liwenga, E., Pradhan, P., Rivera-Ferre, M. G., Sapkota, T., Tubiello, F. N., and Xu, Y. (2019). *Food security*. Intergovernmental Panel on Climate Change.

MPI (2023). Migration data hub. Migration Policy Institute's Migration Data Hub. Accessed on 25 August 2023 at http://www.migrationpolicy.org/programs/migration-data-hub.

Ruggles, S., Flood, S., Sobek, M., Brockman, D., Cooper, G., Richards, S., and Schouweiler, M. (2023). Acs 2016. IPUMS USA: Version 13.0. Accessed on 25 August 2023 at https://doi.org/10.18128/D010.V13.0.

Schlenker, W. and Roberts, M. J. (2009). Nonlinear temperature effects indicate severe damages to u.s. crop yields under climate change. *Proceedings of the National Academy of Sciences*, 106(37):15594–15598.

Tauchen, G. (1986). Finite state markov-chain approximations to univariate and vector autoregressions. *Economics letters*, 20(2):177–181.

US DHS (2022). 2021 yearbook of immigration statistics. Technical report, U.S. Department of Homeland Security, Office of Immigration Statistics, Washington, D.C.

World Bank (2023). World development indicators. Accessed on 25 August 2023 at https://databank.worldbank.org/reports.aspx?source=world-development-indicators.

World Food Program (2015). Initial analysis of the impact of the drought on food security in guatemala, el salvador, and honduras.

A Reduced-form Estimations

A.1 Exposure and Migration Rates

In this exercise, we show the different coefficients of exposure on migration rates by changing the temperature threshold of exposure. Following the same specification as in Equation (1), in Figure A.1, we plot the β_e coefficient for exposure to temperatures above 30, 31, 32, 33, 34, and 35°C. The bands correspond to the 95% confidence interval. Results of the specification can be found in Table A.3 of the Appendix.

Figure A.1: Effect of Exposure on Rural Migration Rates by Temperature Threshold

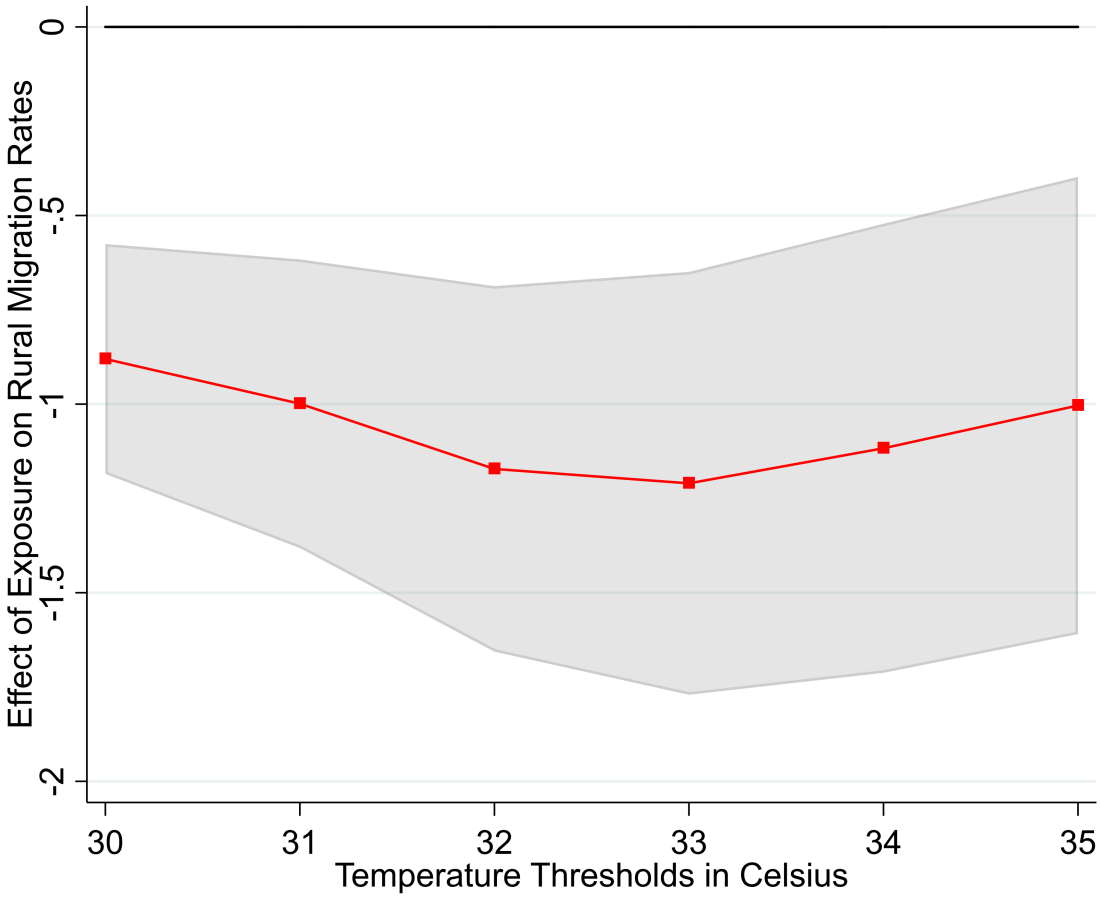

A.2 Link Between Weather and Rural Transitory Shocks

We obtain the link between high temperatures and rural transitory shocks by regressing log yields of corn with exposure during the crop season, March to August for the U.S., using U.S. data. We take the dataset from Schlenker and Roberts (2009) and run the following Fixed-effects regression:

$$y_{cst} = \alpha + \beta_1 Exposure_{cst} + \delta Rain_{cst} + \delta_2 Rain^2_{cst} + \eta_s D^*_s t + \eta_{s2} D^*_s t^2 + \kappa_c + \varepsilon_{cst}$$

Where y_{cst} is the ln yield of corn for county c, state s and year t; $Exposure_{cst}$ is the number of days during the corn crop season a county has been exposed to temperatures above 86F/30C; $Rain_{cst}$ and $Rain^2_{cst}$ is the total precipitation during the season and its quadratic term, respectively; $D^*_s t$ and $D^*_s t^2$ is a state time trend and its quadratic term, respectively; κ_c and η_t are the fixed effect terms for county and year respectively; ε_{ct} is the error term.

Table A.1: Effect of Exposure on Corn yields

Variables	**Corn yields (in logs)**
Exposure to 30C	-0.023***
	(0.001)
Constant	3.619***
	(0.061)
Observations	128,169
R^2	0.850
Precipitation controls	YES
County FE	YES
State time trends	YES

Robust standard errors in parentheses
*** p<0.01, ** p<0.05, * p<0.1

A.3 Other Specification Results

Table A.2: Effect of Exposure on Migration Rate by Percentage of Rural Population

Variables	(1) Mig Rate 0-20%	(2) Mig Rate 20-40%	(3) Mig Rate 40-60%	(4) Mig Rate 60-80%	(5) Mig Rate 80-100%
Lagged Exposure	0.059	-0.540**	-1.026***	-1.040***	-0.906***
	(0.299)	(0.207)	(0.322)	(0.253)	(0.302)
Observations	636	778	1,341	1,630	1,257
R^2	0.072	0.207	0.228	0.309	0.341
Number of Municipalities	38	46	79	96	74
Time and Municipality FE	YES	YES	YES	YES	YES

Note: This table shows the results of the specification in (1), by segmenting the sample according to the share of rural population of each municipality. For example, the first column shows the results of the specification for municipalities that have a share of rural population that is between 0-20%. This table is used as an input for Figure 1. Robust standard errors in parentheses. *** p<0.01, ** p<0.05, * p<0.1

Table A.3: Effect of Exposure on Emigration Rate for Different Temperature Thresholds

Variables	(1) Rural Mig Rate	(2) Rural Mig Rate	(3) Rural Mig Rate	(4) Rural Mig Rate	(5) Rural Mig Rate
Lagged Exposure 30C	-0.880***				
	(0.152)				
Lagged Exposure 31C		-0.999***			
		(0.191)			
Lagged Exposure 32C			-1.172***		
			(0.242)		
Lagged Exposure 33C				-1.210***	
				(0.280)	
Lagged Exposure 34C					-1.117***
					(0.298)
Observations	5,236	5,236	5,236	5,236	5,236
R^2	0.263	0.260	0.258	0.256	0.256
Number of Municipalities	309	309	309	309	309
Time and Municipality FE	YES	YES	YES	YES	YES

Note: This table shows the results of different temperature thresholds. For example, the first column shows the results when the exposure is calculated with a threshold of 30C. This table is used as an input for Figure A.1. Robust standard errors in parentheses. *** p<0.01, ** p<0.05, * p<0.1

B The model through the lens of Caliendo et al. (2019)

In what follows, we provide the interpretation of our model through the lens of the workhorse model in the quantitative dynamic migration models, Caliendo et al. (2019). We focus on the stationary version of the model for simplicity. We proceed by emphasizing the key differences and highlighting in the end why this model cannot explain the data evidence we document.

Key differences. In this version of the model, agents are subject to the same distribution of temporary productivity shocks (or high-heat shocks) than in our baseline model. However, as in Caliendo et al. (2019), agents do not have access to a savings technology, implying $a = a' = 0$, the monetary cost of migration is zero, $m^e = 0$, and but face an additive migration disutility $\tau \geqslant 0$.

Value at the Home Economy. We denote the ex-ante value function as the expectation over the taste shocks as $\mathcal{V}(z, \eta)$. agents at home solve

$$\mathcal{V}(z;\eta) = \mathbb{E}_{\varepsilon}\left[\max\left\{V^s(z;\eta) + \varepsilon^s, V^e(z;\eta) + \varepsilon^e\right\}\right] \tag{9}$$

Value of Staying. Conditional on staying, the agent's value is

$$V^s(z;\eta) = u(wz\eta) + \beta\mathbb{E}\left[\mathcal{V}(z';\eta)\right] \tag{10}$$

Value of Migrating. The value of migrating is the following

$$V^e(z;\eta) = u(wz\eta) - \tau + \beta\left[\mathbb{E}\left[\phi V^*(\eta) + (1-\phi)\mathcal{V}(z';\eta)\right]\right] \tag{11}$$

Value of Living in the U.S.. When the agent is living in the U.S., the value is the following

$$V^*(\eta) = u(c^*)\nu + \beta\left\{\mathbb{E}\left[(1-\psi)V^*(\eta) + \psi\mathcal{V}(z';\eta)\right]\right\} \tag{12}$$

Having the value functions defined, we proceed to set the externally calibrated parameters as in Table 2. Among the two parameters that we estimated, m^e is set to zero by construction and we set ν equal to

1.[26]

Below we conduct the following exercise. We set $\tau \in \mathcal{T} \equiv \{0, 1, 2, \ldots, 48, 49, 50\}$. Solve the policy functions, find the stationary distribution, obtain $1,000$ cohorts of $10,000$ individuals from the stationary distribution, and then run the regression we have in Equation (1) for each cohort and then average out across cohorts, the same approach that we follow for the baseline model. Recalling that β_e is stochastic — i.e., the output of the regression depends on the sample the regression was run on —, we run this exercise 30 times for each $\tau \in T$, record the values for each β_e and report the *range* of these estimates, together with an average. As one expects, with experimentation (not reported), we observe that increasing the number of sampled individuals, cohorts, or experiments makes the average of all these β_e approaches zero for each τ.

Figure A.2: Targeted moments as a function of τ

(a) β_e range for various τ (b) M for various τ

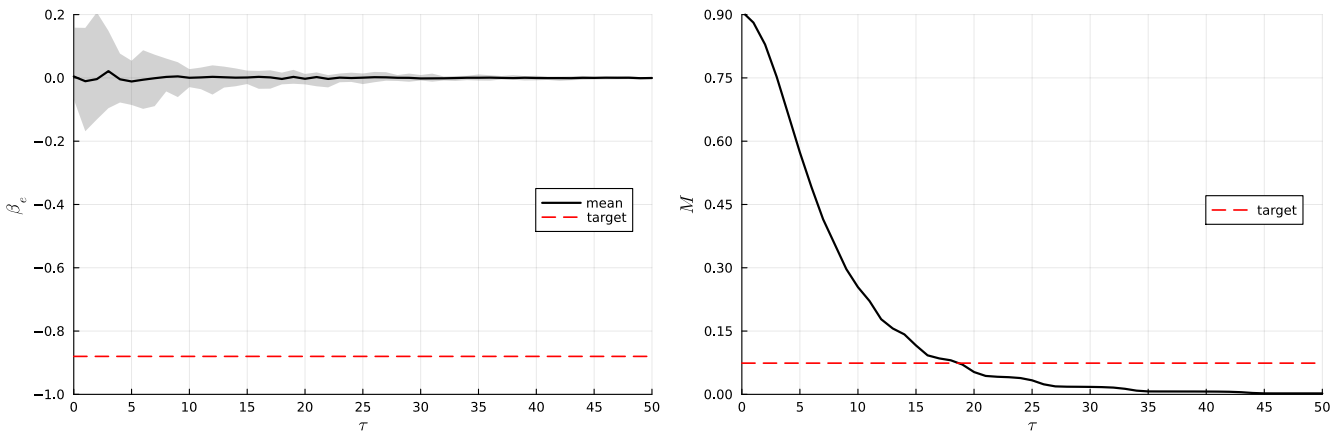

Note: Panel (a) depicts the range of average β_e, over 30 simulations for the average $\hat{\beta}_e$ of 1,000 cohorts of 10,000 agents each. The gray region is the rage, while the black solid line shows the mean over the 30 experiments. Panel (b) exhibits the mass of migrants, M, for each level of τ. This moment is not stochastic — it is computed as a fixed point, as explained in Appendix B. The respective target for each moment is shown as the red dashed line.

Some analysis is due. First, when τ is close to 0, the reference calibration implies that the *variability* of the estimate for β_e is large — the sample used for the regression can make a difference. Observe that M is large when τ is close to 0: the value in the U.S., $V^*(\eta)$ is high relative to $\mathbb{E}[V^s(z, \eta)]$. As τ increases, the value of emigrate decreases and makes the mass of agents in the U.S. get closer to the target of 7.4%.

[26] Clearly, setting ν to the estimated value in our baseline model implies a different *quantitative* result for τ that matches the mass of migrants in the U.S.., but does not modify the *qualitative* conclusions that we layout here, especially regarding the unfeasibility of the model in delivering the correct β_e, other than a "sample coincidence".

But when τ gets higher, the variability of β_e collapses — the value of emigrates shrinks, regardless of the noisy sample one runs the regression, the implied β_e estimate cannot get too far apart from the zero.

Evidently, increasing the number of experiments (30), the number of cohorts (1,000) or sampled individuals (10,000) tends to push the average across experiments closer to 0 in the case of β_e. Hence, we conclude that this version of the model, in the lens of the structure of Caliendo et al. (2019) can, in fact, deliver the share of migrants in the U.S.,M, but not the salient feature of the data, the sensitivity of migration rates to high-heat, or —in the accordance with out mechanism — crop yields, β_e.

C Computational Details

C.1 Solution Method for the Baseline Model

We refer to the Baseline model as the one in which agents do not take into account any Climate Change. We solve the model using standard Value Function Iteration. Since we have the taste shocks for the migrating-staying decision, we do not rely on any type of interpolation.

We start by constructing the set of permanent types, which we denote by η, and assigning a relative share for each node, μ_η. The result is a tuple list $\{\eta^i, \mu_\eta^i\}_{i=1}^{n_\eta}$. Next, we set a grid for assets, A, and a grid for the transitory (weather) shocks, Z.

We set a tolerance $\epsilon = 10^{-10}$ and a relaxation parameter $\xi \in (0,1]$ to allow for slow updating of values, in case $\xi < 1$. [27] We set an iteration counter $t = 1$ and initialize a guess for the value functions as follows

$$\mathcal{V}_t(a,z;\eta) = V_t^e(a,z;\eta) = V_t^s(a,z;\eta) = V_t^*(\eta) = 0.0, \qquad \forall (a,z,\eta)$$

Then we proceed to find policy functions for savings $f_a(a,z;\eta)$, migrating $f_e(a,z;\eta)$ as follows:

1. Update the value of being abroad, $V_{t+1}^*(\eta)$ as

$$V_{t+1}^*(\eta) = u(c^*)\nu + \beta\left[(1-\psi)V_t^*(\eta) + \psi \mathbf{E}_{z'}\left[\mathcal{V}_t(0,z';\eta)\right]\right]$$

2. Compute $V_{t+1}^e(a,z,\eta)$ as

$$V_{t+1}^e(a,z;\eta) = u(wz\eta + a - m^e) + \beta\left[\phi V_t^*(\eta) + (1-\phi)\mathbf{E}_{z'}\left[\mathcal{V}_t(0,z';\eta)\right]\right]$$

3. Compute $V_{t+1}^s(a,z,\eta)$ and $f_{a,t+1}(a,z;\eta)$ as

$$V_{t+1}^s(a,z;\eta) = \max_{a' \in A}\left\{u(wz\eta + a - qa') + \beta \mathbf{E}_{z'}\left[\mathcal{V}_t(a,z';\eta)\right]\right\}$$

[27] In practice, the problem is well-behaved and imposing $\xi = 1$ does not prevent convergence. Otherwise, $\xi < 1$ requires more iterations to converge.

and

$$f_{a,t+1}(a,z;\eta) = \arg\max_{a' \in A} \left\{ u(wz\eta + a - qa') + \beta \mathbf{E}_{z'} \left[\mathcal{V}_t(a,z';\eta) \right] \right\}$$

4. Next, compute $\mathcal{V}_{t+1}(a,z;\eta)$ and $f_{e,t+1}(a,z;\eta)$ as follows [28]

$$\mathcal{V}_{t+1}(a,z;\eta) = \kappa \times \ln \left(\exp\left(\frac{V^e_{t+1}(a,z;\eta)}{\kappa} \right) + \exp\left(\frac{V^s_{t+1}(a,z;\eta)}{\kappa} \right) \right)$$

and

$$f_{e,t+1}(a,z;\eta) = \frac{\exp\left(\frac{V^e_{t+1}(a,z;eta)}{\kappa} \right)}{\exp\left(\frac{V^e_{t+1}(a,z;\eta)}{\kappa} \right) + \exp\left(\frac{V^s_{t+1}(a,z;\eta)}{\kappa} \right)}$$

5. Check for convergence:

   (a) if $\|\mathcal{V}_{t+1}(a,z;\eta) - \mathcal{V}_t(a,z;\eta)\|_\infty \leqslant \epsilon$, abort — the solution was found.

   (b) if $\|\mathcal{V}_{t+1}(a,z;\eta) - \mathcal{V}_t(a,z;\eta)\|_\infty > \epsilon$, update the ex-ante value function as

$$\mathcal{V}_{t+1}(a,z;\eta) \equiv \xi \times \mathcal{V}_{t+1}(a,z;\eta) + (1-\xi) \times \mathcal{V}_t(a,z;\eta)$$

   replace the indexer t by $t+1$ and go back to step 1.

C.2 Computing the Stationary Distribution

Once we find the policy functions for savings and migrating, we compute the stationary distribution as follows.

We initialize from an arbitrary distribution $(\mu_t(a,z;\eta), M_t(\eta))$ (that has to be conformable with $\{\mu^i_\eta\}_{i=1}^{n_\eta}$), we compute the next-period distribution $(\mu_{t+1}(a,z;\eta), M_{t+1}(\eta))$ by applying the tautologies

[28] To render the computation numerically stable, we apply in reality

$$\mathcal{V}_{t+1}(a,z;\eta) = V_{\max} + \kappa \times \ln \left(\exp\left(\frac{V^e_{t+1}(a,z;\eta) - V_{\max}}{\kappa} \right) + \exp\left(\frac{V^s_{t+1}(a,z;\eta) - V_{\max}}{\kappa} \right) \right)$$

with $V_{max} \equiv \max\left\{ V^s_{t+1}(a,z;\eta), V^e_{t+1}(a,z;\eta) \right\}$ and, for the migrating policy function,

$$f_{e,t+1}(a,z;\eta) = \frac{1}{1 + \exp\left(\frac{V^s_{t+1}(a,z;\eta) - V^e_{t+1}(a,z;\eta)}{\kappa} \right)}$$

below:

$$M_{t+1}(\eta) = M_t(\eta)(1-\psi) + E_t(\eta)\phi$$

where

$$E_t(\eta) = \sum_{a\in\mathcal{A}}\sum_{z\in\mathcal{Z}} \mu_t(a,z,\eta) f_e(a,z;\eta)$$

and

$$\mu_{t+1}(a',z',\eta) = \sum_{a\in\mathcal{A}}\sum_{z\in\mathcal{Z}} \mu_t(a,z,\eta)\mathbb{1}\left\{f_{a'}(a,z;\eta)=a'\right\}(1-f_e(a,z;\eta))\Pr(z')$$
$$+\mathbb{1}\left\{a'=0\right\}\Pr(z')\left[M_t(\eta)\psi + E_t(\eta)(1-\phi)\right]$$

We proceed iteratively until the following condition is met

$$\|\mu_{t+1}(a,z;\eta) - \mu_t(a,z;\eta)\|_\infty + \|M_{t+1}(\eta) - M_t(\eta)\|_\infty \leqslant 10^{-6}$$

Our initial guess is given by $M_0(\eta) = 0.0$ and $\mu_0(0,z,\eta) = \Pr(z)\times\mu_\eta$. There is nothing in particular to this guess, any arbitrary (conformable) distribution would converge to the same distribution, up to the numerical inaccuracy tolerated.

C.3 Details on Grids

Permanent productivity, η. In our analysis, we impose $\ln(\eta) \sim N(\mu_\eta, \sigma_\eta^2)$. We chose $n_\eta = 17$ as the number of grid points. We set the lowest η to $\exp(\mu_\eta - 3\sigma_\eta)$, while the highest η is given by $\exp(\mu_\eta + 3\sigma_\eta)$, and choose the intermediary points equally distant from each other (in logs) with using the procedure proposed by Tauchen (1986). Figure A.3 shows the resulting grid together with the mass of agents of each type, under the baseline parametrization.[29]

Asset grid, A. Since we do not rely on interpolating, we choose a $n_a = 100$ as grid points. We set the lower bound to A as the 0.0 and the upper bound as $\max\{A\} = 10.0$, by experimentation.[30] We choose

[29] For each type η, the mass μ_η will be, in the stationary distribution, either domestically or abroad.

[30] Aiming at making sure we get $\max\{A\} > \sup\{f_a(a,z;\eta)\}, \quad \forall(a,z,\eta)$ for possibles combinations of parameters in the estimation procedure.

Figure A.3: Permanent productivity grid

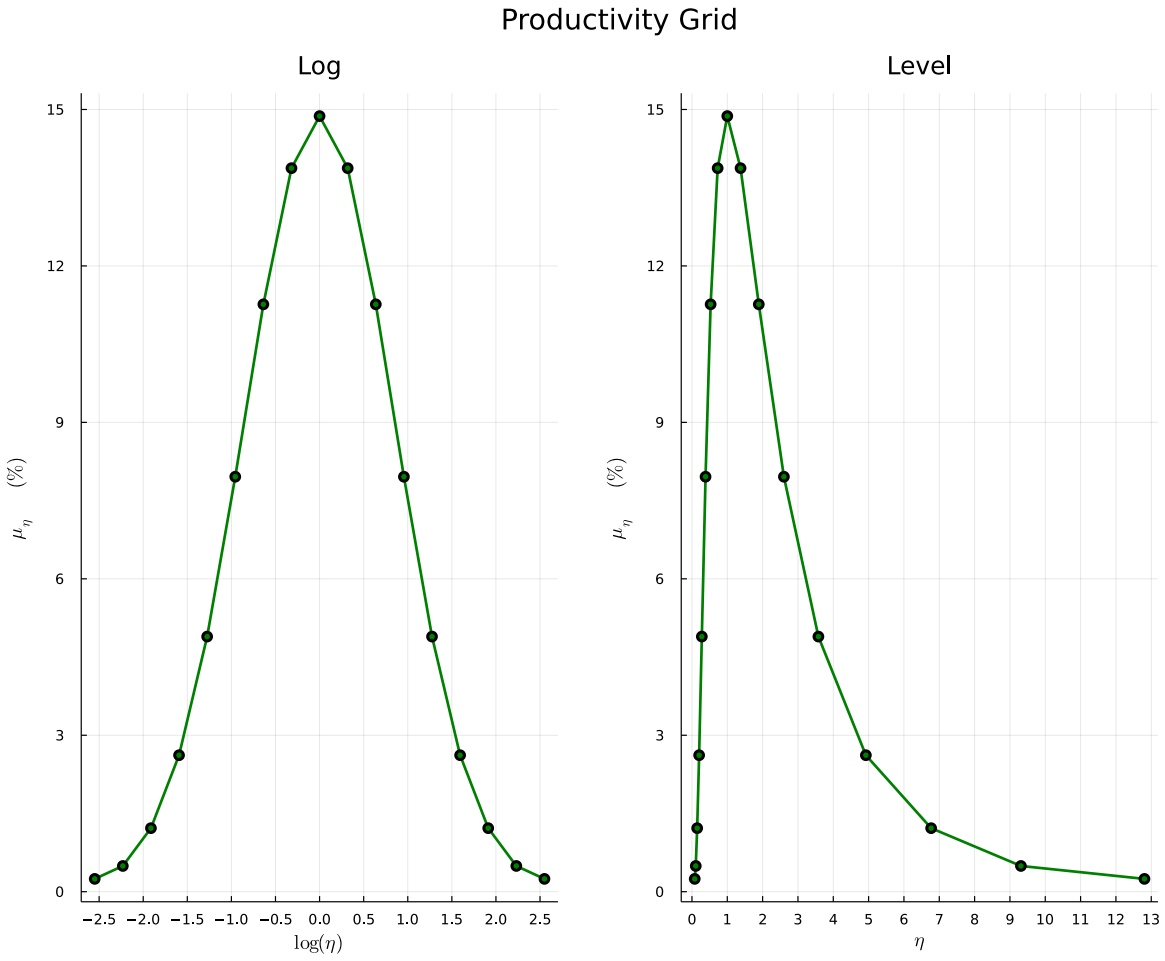

the grid points to be more concentrated around the lower bound, where even small differences in asset holds can give substantial increases in utility.

We choose the following scheme to distribute the grid points. We start by splitting the interval $[0,1]$ as follows (equally spaced points)

$$\left\{ x_j \quad : \quad x_j \equiv \frac{j-1}{n_a - 1}, \quad j = 1, 2, \ldots, n_a \right\}$$

Then we set a parameter $\theta = 2.25$ and compute the A grid as follows, for $j \in \{1, 2, \ldots, n_a\}$

$$a_j = a_{\min} + (a_{\max} - a_{\min}) x_j^{\theta}$$

Figure A.4 shows the asset grid for our baseline specification — $\theta = 2.25$ — and two other alternatives. Given $\theta > 1$, there are more grid points around $a_{\min}$ than around $a_{\max}$. If $\theta = 1$, then the asset grid would be just linearly spaced. If instead $\theta = 3.5$, we would observe even more grid points around $a_{\min}$.

Figure A.4: Asset grid

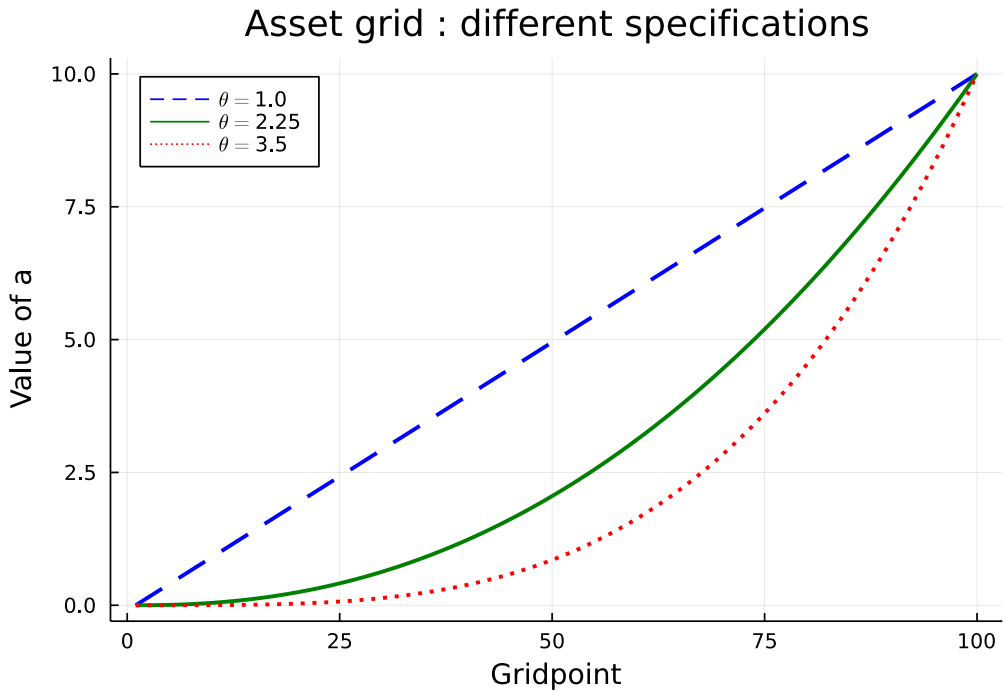

High Temperature Shocks, Z. To build our Z grid, first, we obtain the distribution of exposure at the municipality-year level for the period of analysis 2011-18. Second, we calculate the CDF weighted by the

rural population of the municipality. Third, from the CDF, we compute the probability of having 0 days of exposure and the following intervals: (0,2], (2,5], (5,10], (10,20], (20,35], and more than 35. This sets our number of grid points for Z to 7, i.e., $n_Z = 7$. Once the probabilities are calculated, we compute the weighted average of exposure for 0 days and every interval. Ultimately, we calculate the corresponding Z according to Equation (4). The probability for every Z point is the one calculated in the third step.

D Estimation of σ_η

D.1 Main Estimation

To obtain the value of σ_η we estimate rural yields from farmers in Guatemala. For this we use microdata from the last agricultural census in Guatemala "IV Censo Nacional Agropecuario 2003", corresponding to the crop year 2002–03 conducted by the National Statistical Institute (INE). The census includes information on quantities produced, labor, land size, input use, machinery and equipment, as well as geographic location, however, it does not include any information on prices, sales or costs.

Given we only observe quantities produced, we obtain data on market prices of several crops for the year 2003 from the Ministry of Agriculture, Livestock and Food. We compute the total revenue of the farm by multiplying the market prices to each crop and adding them up by producer. Then, we divide the revenue by total harvested area in hectares and total labor employed by the producer. Because we do not have data on the cost or use intensity of intermediate inputs, only if they were used in production, we estimate eta_i as the residual of the following reduced-form estimation

$$\ln(\text{rev}_{ip}) = \gamma X_i + \alpha_p + \ln(\eta_i) \tag{13}$$

where rev_{ip} is the total revenue per hectare and labor of producer i; X_i is a vector of controls and inputs which are included the household over total labor ratio, if the producer has machinery, equipment, uses high-performance seeds, organic and chemical fertilizer, if it has irrigation and number of cultivated crops; α_p is the fixed-effect term for populated place which is a subdivision of municipality. The results of the regression can be seen in Table A.4. After recovering the residual, we calculate the standard deviation which is equal to 0.71.

D.2 Alternative Estimation

Considering the lack of data regarding cost of intermediate inputs, we estimated the value of σ_η using the 2014 National Survey of Living Conditions (ENCOVI) compiled by INE. This is a household survey representative at the national level. The dataset includes a module detailing agricultural production with

Table A.4: Regression estimating η_i

Variables	**Revenue (in logs)**
Household Labor/Total Labor	1.110***
	(0.035)
If has machinery	-0.047***
	(0.016)
If has equipment	-0.027***
	(0.009)
If uses high-performance seeds	-0.010
	(0.015)
If uses organic fertilizer	-0.026***
	(0.008)
If uses chemical fertilizer	-0.043*
	(0.023)
If uses pesticide	-0.008
	(0.016)
If has irrigation system	0.022
	(0.017)
Number of crops	-0.418***
	(0.019)
Observations	580,267
R-squared	0.561
Populated Place FE	YES

Robust standard errors in parentheses
*** p<0.01, ** p<0.05, * p<0.1

information on quantities produced, sales, labor, land size, input use, and costs.

To estimate η_i, first we compute the value added of production. Given problems with outliers, we calculate the implicit sale price for each crop, dividing total sales (in Quetzales, the Guatemalan currency) by total quantities sold. After that, we multiply the price by the total quantities produced for every crop, ultimately adding all the crops and resulting in total revenue. Then we proceed to subtract intermediate inputs costs involved in the crop production. These inputs include seeds or plants, organic and chemical fertilizers, pesticides, packaging, and fuel.

After obtaining the value added, we divide it by total land, and by the implicit labor cost. As most producers employ family members for agricultural activities, we calculate the median profits of producers and take this as the implicit wage of producer, and any household member that reports working at the establishment, as their main job. We finally add any hired labor wages to the total implicit wage, to have our measure of implicit labor cost.

Lastly, we estimate η_i as the residual of the following regression

$$\ln\left(value\ added_{ij}\right) = \alpha_j + \ln\left(\eta_i\right) \tag{14}$$

where $value\ added_{ij}$ is the value added per hectare and labor cost of producer i in department j; α_j is the Fixed Effects term at department-area level.[31] When we recover the residual, the standard deviation is equal to 0.81, higher than our estimate from the agricultural census.

[31] Data on municipality is not available, department is a geographical administrative level above municipality. Area refers if the household is located in a rural or an urban setting.

E Simulated Method of Moments

E.1 Computing the Stationary Distribution

In our model, a unitary mass of agents is split between either in the Home economy or abroad. Let $\mu(a,z,\eta)$ be the mass of agents at Home with the state vector (a,z,η), and $M(\eta)$ the mass of agents abroad with innate productivity η. Agents abroad do not carry any asset a, and their value is independent of the temporary idiosyncratic shock z that affects the rural production in the Home economy.

Given a current distribution of agents, i.e., the pair $(\vec{\mu},\vec{M}) \in \mathcal{D} \subset \mathbb{R}^3_+ \times \mathbb{R}$, the transitory shock distribution, say $\{(z,\Pr(z))\}_{z\in\mathcal{Z}}$, the exogenous probability of deportation ψ, and the success rate of migration ϕ, we can write the law of motion of distribution of agents as[32]

$$M'(\eta) = M(\eta)(1-\psi) + E(\eta)\phi \tag{15}$$

where

$$E(\eta) = \sum_{a\in\mathcal{A}}\sum_{z\in\mathcal{Z}} \mu(a,z,\eta) f_e(a,z,\eta) \tag{16}$$

and

$$\begin{aligned}\mu'(a',z',\eta) = \sum_{a\in\mathcal{A}}\sum_{z\in\mathcal{Z}} \mu(a,z,\eta)\mathbb{1}\left\{f_{a'}(a,z,\eta)=a'\right\}(1-f_e(a,z,\eta))\Pr(z') \\ +\mathbb{1}\left\{a'=0\right\}\Pr(z')\left[M(\eta)\psi + E(\eta)(1-\phi)\right]\end{aligned} \tag{17}$$

Equations (15)-(17) define implicitly an operator $\mathcal{T}: \mathcal{D} \mapsto \mathcal{D}$. We call a stationary distribution an element $(\vec{\mu},\vec{M}) \in \mathcal{D}$ such that $\mathcal{T}\left((\vec{\mu},\vec{M})\right) = (\vec{\mu},\vec{M})$, that is a fixed-point of $\mathcal{T}$.

Equation (15) shows that for the following period, the mass of agents equipped with a particular productivity level η that will be abroad, $M'(\eta)$, is given by the agents that are currently abroad $M(\eta)$ times the probability of not being deported $(1-\psi)$ plus the mass of agents that successfully migrated in the current period and will be abroad next period, $E(\eta)\phi$.

[32] In particular, for the migrating policy function, the law of large numbers gives that the probability of migration is equal to the proportion of agents migrating, condition on a triplet state.

Equation (16) shows the definition of agents that tried to migrate in the current period. By the law of large numbers, a fraction ϕ of them will be abroad next period, while the remaining fraction $1-\phi$ will be detained and sent back to the Home economy. It is the sum of the mass of agents with assets a, temporary productivity z, and permanent productivity η, $\mu(a,z,\eta)$, times the migration probability, $f_e(a,z,\eta)$.

Equation (17) is the stock of agents in the Home economy with a state vector (a',z',η). There are two elements. The first term consists of agents that are in the Home economy and do not migrate, which happens with probability $1-f_e(a,z,\eta)$, and have chosen $f_{a'}(a,z,\eta)=a'$, and drawing transitory productivity z', which happens with probability $\Pr(z')$, taking into account the initial mass $\mu(a,z,\eta)$. The second term is the mass of agents that were deported and are sent back with zero assets —$a'=0$, $M(\eta)\psi$, times the probability of drawing the transitory productivity z', $\Pr(z')$. In addition, there is a mass of agents that tried to migrate but failed, $E(\eta)(1-\phi)$.

As we discussed, we use the stationary distribution to estimate some parameters of the model. In addition, the stationary distribution of agents is a helpful tool for analyzing *terminal* outcomes under climate change projections after any transition dynamics is concluded.

E.2 Procedure

Let θ be the $p\times 1$ vector of parameters to be estimated. Let g_d be the $m\times 1$ vector of moments in the data that we want to replicate and $g(\theta)$ the $m\times 1$ vector counterpart of these moments as a function of the parameter vector θ.

We define the vector of of model error as the gap between the model implied moments $g(\theta)$ and the corresponding vector of moments from the data g_d:

$$e(\theta)\equiv g(\theta)-g_d \tag{18}$$

The loss function we consider is

$$\mathcal{L}(\theta)\equiv e(\theta)^T\mathcal{W}e(\theta) \tag{19}$$

where $\mathcal{W}$ is a $m\times m$ positive semi-definite matrix of weights. Observe that $\mathcal{L}:\Theta\mapsto\mathbb{R}_+$. The objective is

to find a vector θ^* in a space Θ that attains the minimum of the loss function, that is:

$$\theta^* \in \arg\min_{\theta \in \Theta} \mathcal{L}(\theta) \tag{20}$$

E.3 Implementation

In our implementation, we estimate two parameters and target two moments, that is $p = 2$ and $m = 2$. Hence, the system is identified. The parameters that we estimate are $\theta \equiv [m^e, \nu]$.

We implement the Nelder-Mead algorithm with $(p+1)$ (randomly chosen) vectors as an initial simplex to minimize the loss function. We set the weighting matrix $\mathcal{W}$ to be the identity matrix.

We experiment with some combinations of θ to figure out a tentative candidate for the argument that minimizes the loss function. Then, we create a large interval for each parameter around this tentative solution to construct a parameter space for the Nelder-Mead search. We set the parameter space Θ for the search as a box. The relevant space Θ is the Cartesian product over these intervals.

Table A.5: Interval allowed for each parameter

Parameter	θ_i^{lb}	θ_i^{ub}
m^e	$1 \times \mathbb{E}[z]$	$3 \times \mathbb{E}[z]$
ν	1.0	3.0

Note: θ_i^{lb} and θ_i^{ub} stand for the lower-bound and upper-bound, respectively, for parameter θ_i.

Yielding $\Theta \equiv [1 \times \mathbb{E}[z], 3 \times \mathbb{E}[z]] \times [1.0, 3.0]$.

The Nelder-mead algorithm is implemented *without* any constraints. To achieve that, we performed a logistic transformation over each interval, for each parameter, according to the formula[33]:

$$y_i(x) = \theta_i^{lb} + \frac{1}{1+\exp(-\lambda x)}(\theta_i^{ub} - \theta_i^{lb}), \qquad \lambda > 0$$

implying

$$\lim_{x \to -\infty} y_i(x) = \theta_i^{lb} \qquad \text{and} \qquad \lim_{x \to +\infty} y_i(x) = \theta_i^{ub}$$

[33] In our implementation we set $\lambda = 1$.

Defining the map that performs the logistic transformation as

$$H(y) : \mathbf{R}^2 \mapsto \Theta$$

we rewrite the loss function as

$$\tilde{\mathcal{L}} : \mathbf{R}^2 \mapsto \mathbf{R}_+$$

explicit as the composition $\tilde{\mathcal{L}} = (\mathcal{L} \circ H)(y) \equiv \mathcal{L}(H(y))$. The problem we input to the Nelder-Mead algorithm is then

$$\min_{y \in \mathbf{R}^2} \tilde{\mathcal{L}}(y)$$

Once a candidate solution is found for the minimum, $y^* \in \mathbf{R}^2$, we applied the logistic transformation to figure out the relevant parameter factor that gives the minimum, i.e, $\theta^* \equiv H(y^*)$.

E.4 Dealing with the Stochastic β_e

As in the main specification from the empirical part, we got a connection between high heat and migration. In disciplining the model, we explicitly build the link between weather conditions and rural productivity. In the model, we get a connection between rural productivity and migration probability. To get in the model a regression, such as in the data, of migration rate on the high-heat shocks, we proceed as follows. We first solve the model given a vector of parameters and find the stationary distribution. Next, we draw $1,000$ samples of $10,000$ individuals indexed by i from it and run the following regression:

$$f_e(a, z, \eta)_i = \gamma_0 + \gamma_1 \log(z_i) + \epsilon_i \tag{21}$$

where $f_e(a, z, \eta)$ is the migration probability under state (a, z, η). In what follows, we let the estimate of γ_1 under sample s to be $\hat{\gamma}_s$. Intuitively, the value of $\hat{\gamma}_s$ should be positive. A higher temporary productivity (i.e., higher z) relaxes the budget constraint and makes it more likely to afford the migration cost. It also increases the value of staying. As in general, $c^s(a, z, \eta) \gg c^e(a, z, \eta)$, the valuation of an extra unit of resources is higher under migrating than staying, and thus, a higher z tends to increase the probability of migrating.

The value of $\hat{\gamma}$ that feeds in the loss function in Equation (19) is the average of the $1,000$ estimates, one for each sample. That is, denoting a sample by $s \in \{1,2,\ldots,1000\}$, we input in the loss function

$$\gamma = \frac{1}{1000}\sum_{s=1}^{1000}\hat{\gamma}_s$$

To make g_d comparable to this $\hat{\gamma}$, we convert the estimated coefficient in the regression in Table 1 into the effect of one extra day of exposure above 30°C/86°F in the productivity, according to

$$\ln(z) = \ln(1-\chi)\times h \tag{22}$$

where $\chi = 0.023$ is the estimated average decrease in the yield for an extra day of exposure to a temperature above 30°C/86°F. Hence

$$\frac{\partial \ln(z)}{\partial h} = \ln(1-\chi) \tag{23}$$

and so the target for the parameter γ is, adjusting per the success rate of migration, ϕ:

$$g_d \equiv \frac{\hat{\beta}_e}{10,000}\frac{1}{\phi}\frac{1}{\ln(1-\chi)} \tag{24}$$

It is important to recall that the definition of the migration rate reported in Table 1 is per 10,000 individuals. Hence, we need to adjust the estimated value to according to the normalization. We adjust by the success rate of migration since we only observe in the data the effective migration, not the attempts to migrate.

E.5 Sampling from the stationary Distribution

When estimating the model, we collected 1,000 samples of 10,000 individuals from the stationary distribution to compute the regression coefficient $\hat{\gamma}$ from Equation (21) from the main text. In this appendix, we show a checker on the sampling procedure. These individuals are sampled from the mass of households that are "currently" in Guatemala, that is $\mu(\cdot)$ rather than $M(\cdot)$.

From the stationary distribution in the baseline model, we derive the implied flow of households as

$$E \equiv \sum_{\eta} E(\eta) = \sum_{\eta} \sum_{a} \sum_{z} \mu(a,z,\eta) f_e(a,z;\eta)$$

Alternatively, it is easy to show that, in the stationary distribution,

$$E = \frac{\psi}{\phi} \times M \equiv \frac{\psi}{\phi} \times \sum_{\eta} M(\eta)$$

From regression (21), its counterpart in the regression is given by

$$E_{\text{reg}} \equiv (\hat{\gamma}_0 + \hat{\gamma}_1 \mathbb{E}[\ln(z)])$$

In reality, we need to multiply the number by

$$\sum_{\eta} \sum_{a} \sum_{z} \mu(a,z,\eta),$$

an adjustment to take into account that, in the stationary distribution, the mass of agents in the home economy does not sum to 1. The remaining fraction is abroad, in the U.S.

Figure A.5 below shows the model implied flow of tentative migrants from the stationary distribution, with the dotted black line and its counterpart implied by the regression. The former is computed without sampling and does not depend on the sample size.

The implied flow computed from the regression does depend on the particular sample. The plot shows in the x-axis an increasing (in log_{10} scale) the sample size. Then, for 1000 samples in total, we computed the implied emigration flow from each regression, given a sample size, and restored the results. Then, we compute 5 and 95 percentiles and the mean. The plot shows that as the sample size grows, the implied flow from the regression converges to the one computed directly from the stationary distribution.

The punchline is that the sampling from the stationary distribution is not flawed.

Figure A.5: Implied mass of agents trying to Emigrate

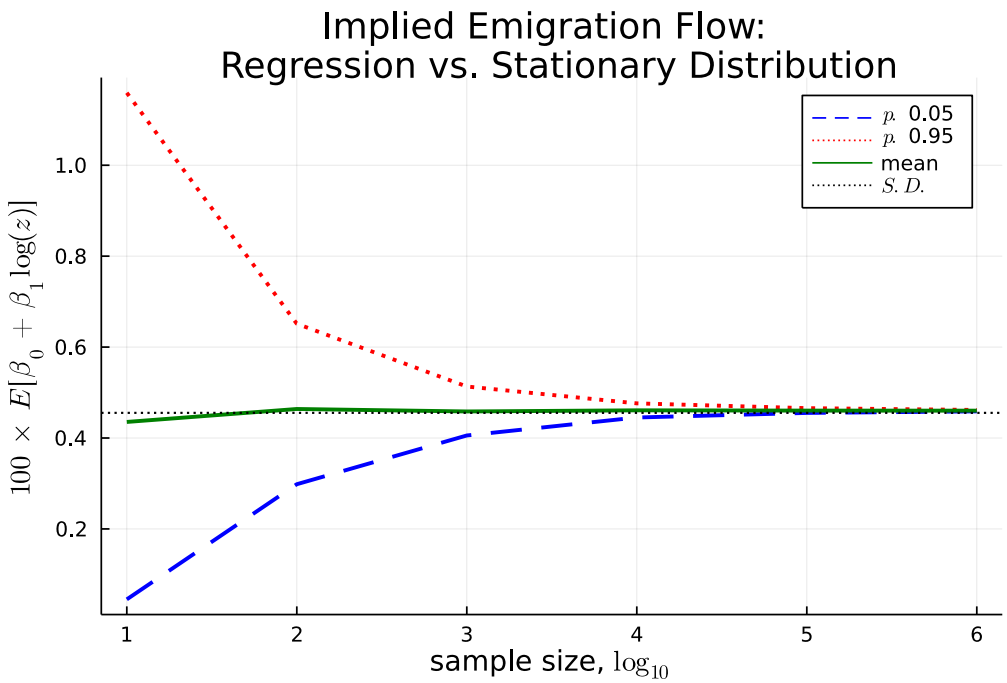

Note: The dotted black line shows the implied (tentative) emigration flow from the stationary distribution, which does not rely on sampling. The regression we run to estimate the model does rely on sampling. The plot shows the lines for the sampling exercises. For each sample size, in the x-axis, we sample 300 samples, run the regression, and collect the implied, by each regression, the tentative emigration flow. Then, with the data from the 300 samples, we compute the 5 and 95 percentiles in blue and red, respectively. The mean over is in solid green.

F Climate Change Transitions

F.1 Data

In this section, we explain in more detail how we construct the transitory productivity grid points and their respective probabilities. Figure A.6 shows the increases in temperature projected for each scenario and its quadratic fit, as we discussed in the main text. We take these projections and calculate the quadratic fit for every scenario as follows:

$$P_t = \alpha + \beta_1{}^* t + \beta_2{}^* t^2 + \varepsilon_t \tag{25}$$

Figure A.6: Temperature Increase by Climate Change Scenario

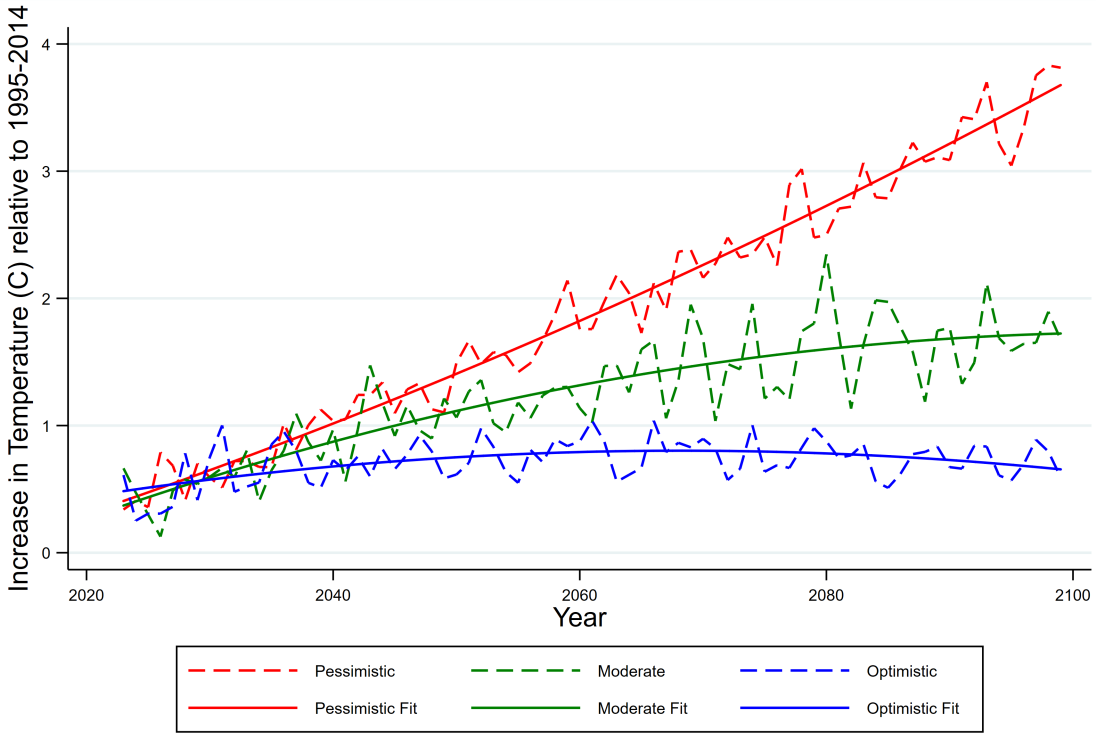

To get the Z grid points along the transition, we compute them in a similar fashion as our baseline Z grid for every projected year. First, we take the satellite temperature data from Copernicus Climate Change Service (2019) at the raster-hourly level for the 1995-2014 period, and we add the quadratic fit estimated in (25), $\widehat{P}_t$. Second, we calculate the exposure to temperatures above 30°C during the main crop season and collapse the raster level projections into the municipal level, as described in Section 2 of the paper. Third, we compute our Z points and the respective probabilities as in Section C.3 of the Appendix.

We apply this procedure for every projected year from 2023 to 2100. After 2100, we assume temperatures are the same for every scenario. Therefore, the Z grid after 2100 is the same as in 2100. In Figure A.7, we plot the histogram for the distribution of exposure for our baseline and for the different climate change scenarios in the year 2100. As we can see, the distribution for the optimistic case is similar to our baseline, while for the moderate case, we see a shift towards more exposure days. For the pessimistic case, the shift is more pronounced as the probability of experiencing many days above 30°C increases.

Figure A.7: Exposure Distribution for Baseline (1995-2014) and by Scenario in 2100

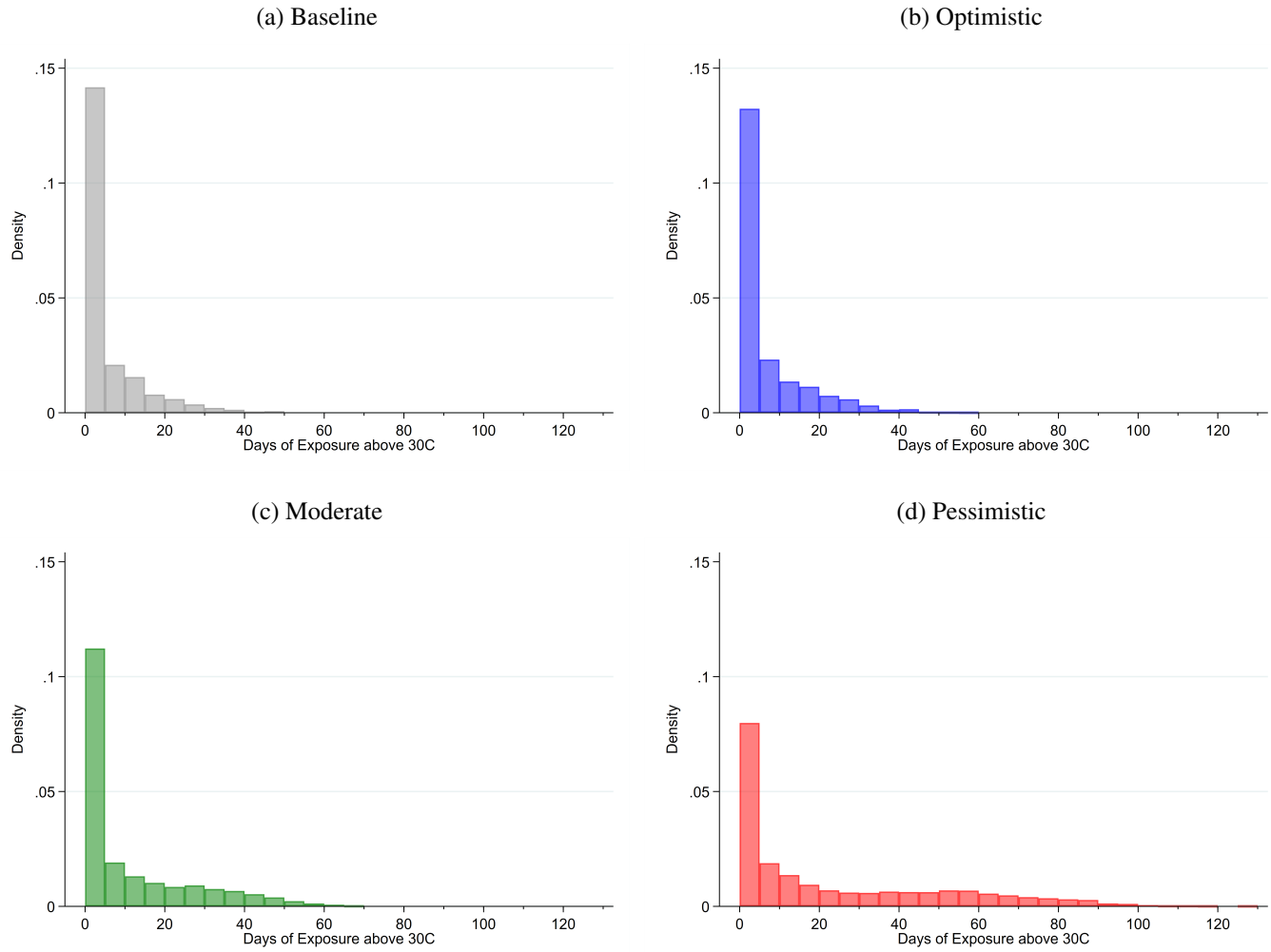

F.2 Model

F.2.1 Forward-looking agents

This is our main exercise. For agents that are forward-looking, we assume that agents have Rational Expectations and learn at date $t = 0$, still under the baseline distribution of the weather shocks, the whole path for the transitory shocks, $\mathcal{Z}$. This is a perfect foresight exercise regarding the path of distributions.

In order to solve the value functions, policy functions, and distributions *along* the transition, we follow these steps:

1. Solve the Value Functions and Policy Functions at date $t = T$ as if the shocks were to be forever as in the last period of the transition.

2. Starting at $t = T$, set the Continuation Values as $V_t^*(a, z; \eta)$ and $\mathcal{V}_t(a, z; \eta)$

3. From $t = (T-1)$ to $t = 0$, decreasing one by one the time iterator t, use the appropriate distribution of shocks at date t, $\mathcal{Z}_t$, to solve **backward** the sequence of Value Functions and Policy Functions.

4. Having found the **complete** sequence of policy functions, iterate **forward** to using the policy functions, the adequate $z \to z'$ transitions, and the initial distribution of agents, to compute the mass of agents in the *Home* economy, the mass of agents trying to emigrate and the mass of agents abroad.

After completing all these steps, we own the following objects.

Value Functions.

$$\{V_t^e(a, z; \eta), V_t^e(a, z; \eta), \mathcal{V}_t(a, z; \eta), V_t^*(\eta)\}_{t=0}^T$$

Policy Functions.

$$\{f_{a,t}(a, z; \eta), f_{e,t}(a, z; \eta)\}_{t=0}^T$$

Distribution of Agents and Flow of Tentative Migrants.

$$\{\mu_t(a, z, \eta), M_t(a, z, \eta), E_t(a, z, \eta)\}_{t=0}^T$$

After $t = T$, all these objects will be equal to the baseline model computed under the appropriate distribution of shocks, which is $\mathcal{Z}_T$.

F.2.2 Non-Forward Looking Agents

For the case of non-forward looking agents, we assume that they do observe the *entire* distribution of shocks at (and up to) date t, but they *expect* to have the current (period by period) distribution going forward. Our preferred interpretation is that they believe in what they see, but think the future is not going to get worse. In this sense, they are backward-looking agents.

There is one main difference relative to the case agents having perfect foresight regarding the future productivity distribution's path. Period by period along the transition, we update the current realization of shocks. Then, using similar steps to B, we compute the fixed-point value functions to get the continuation value for the households, using the current distribution of transitory shocks as "permanent". Equipped with these continuation values, we then solve for the policy functions period by period.

G Additional Results

G.1 Stock of Migrants

Figure A.8: Effect of Climate Change on Stock of Migrants

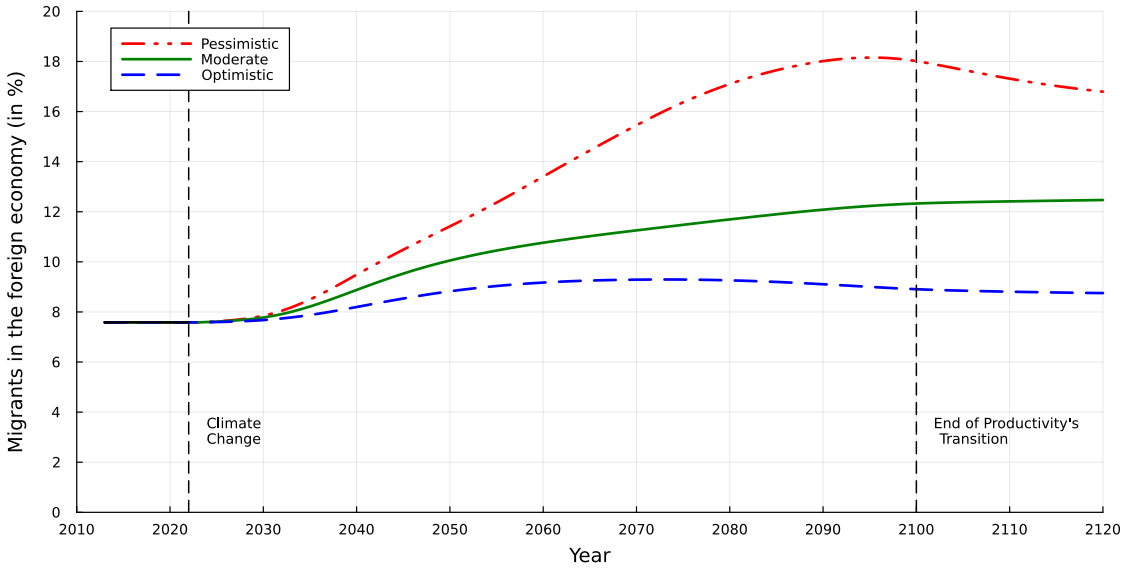

Figure A.9: Effect of Anticipation on Stock of Migrants

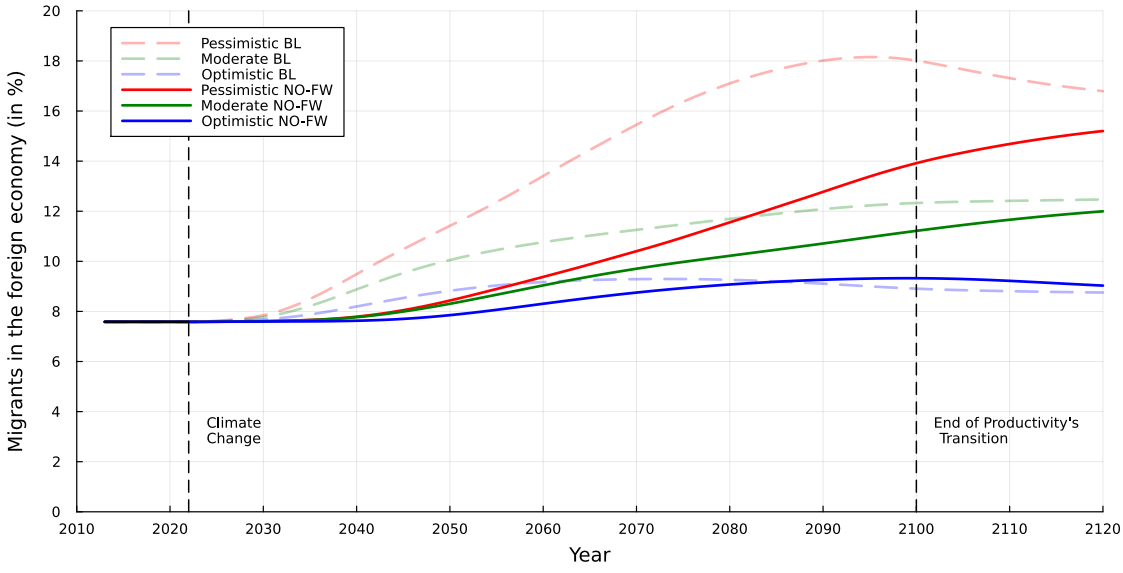

G.2 Stationary Distributions

Figure A.10: Stock of Migrants by Productivity at the Initial and Final stationary state for each Scenario

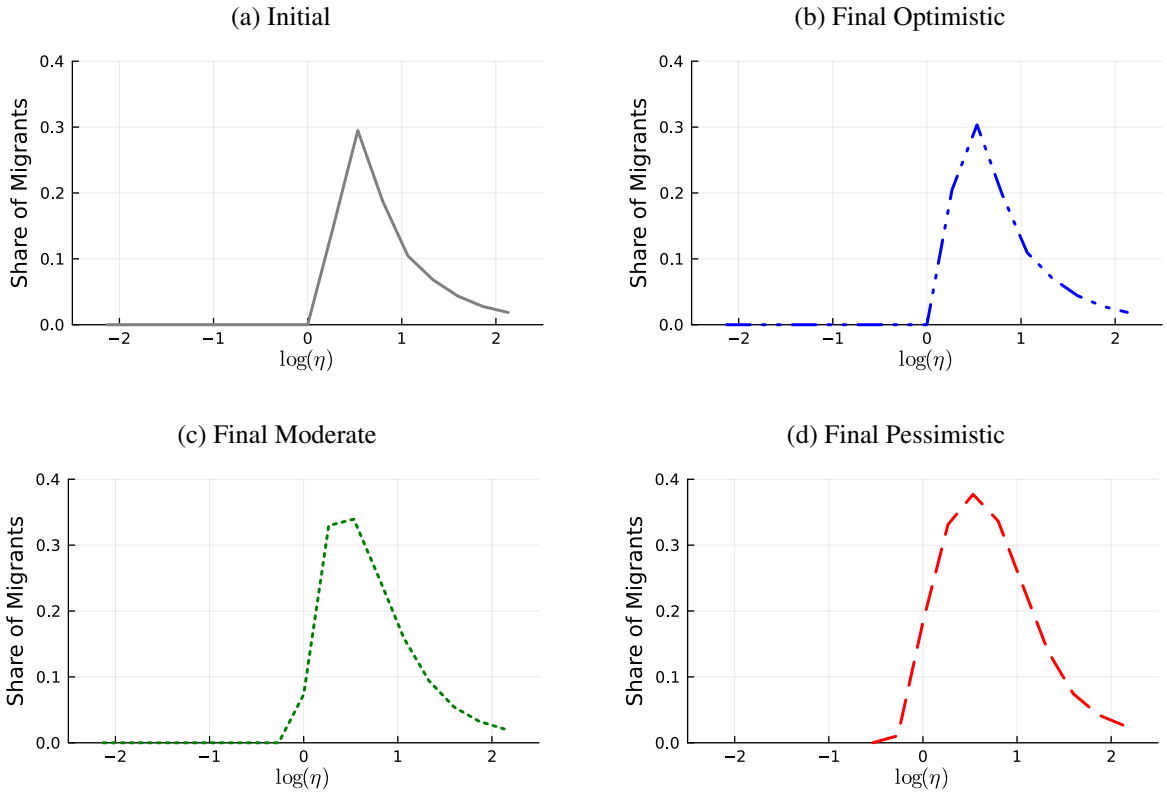

Figure A.11: Final Asset PDF at the Initial and Final stationary state for each Scenario

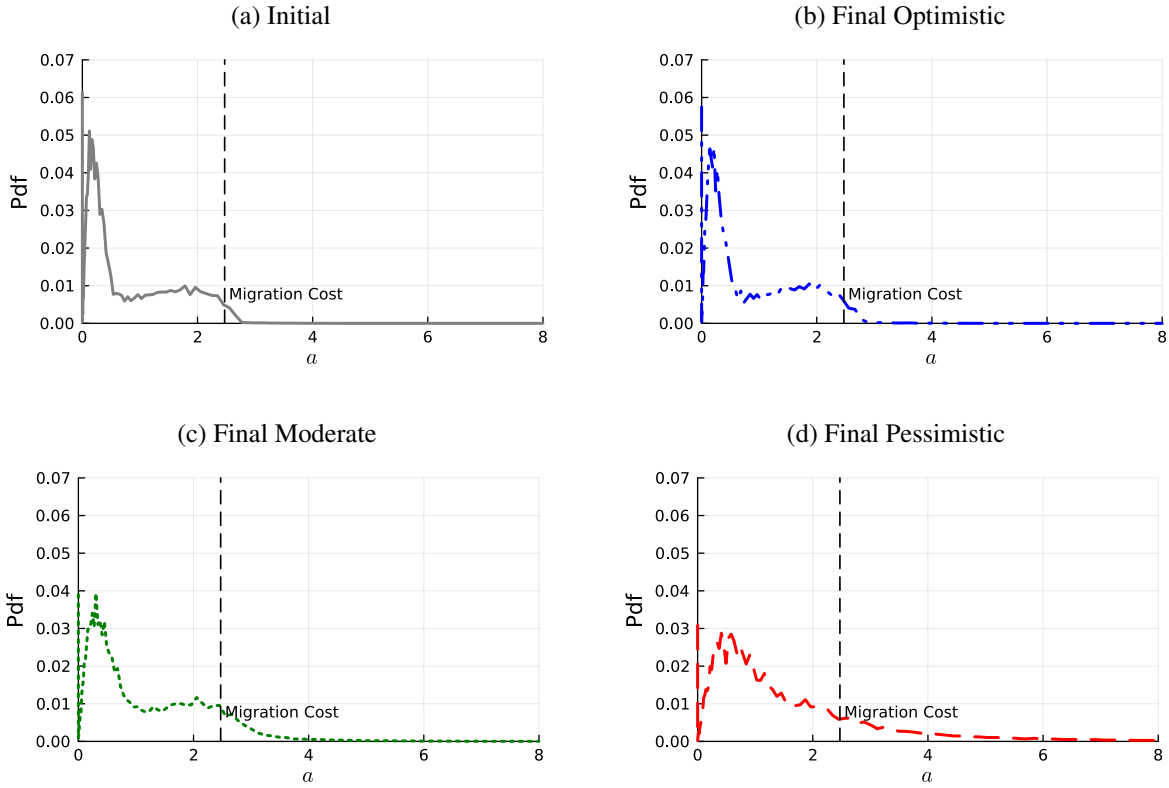

Figure A.12: Stock of Migrants by Productivity for each Scenario and UCT scheme at the Final stationary state

(a) Optimistic, Universal Cash Transfer

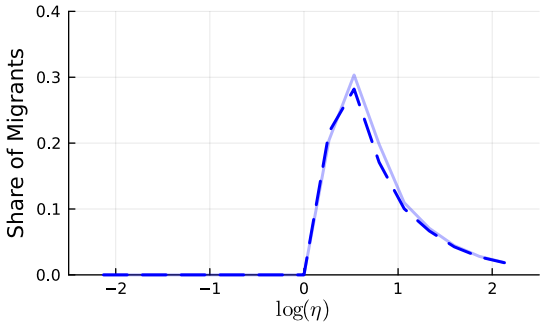

(b) Optimistic, High-Heat Cash Transfer

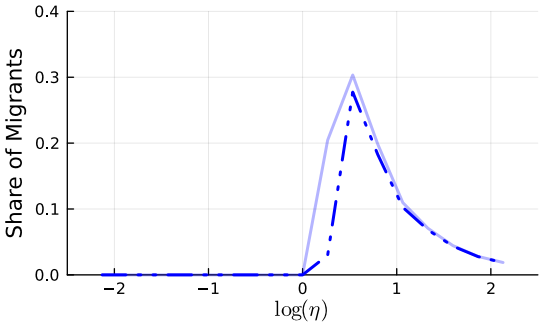

(c) Moderate, Universal Cash Transfer

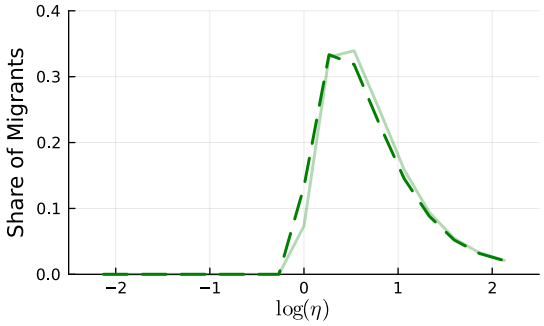

(d) Moderate, High-Heat Cash Transfer

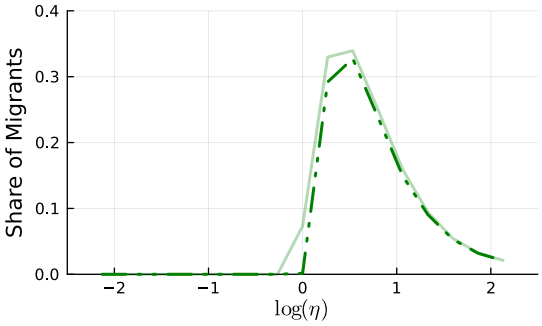

(e) Pessimistic, Universal Cash Transfer

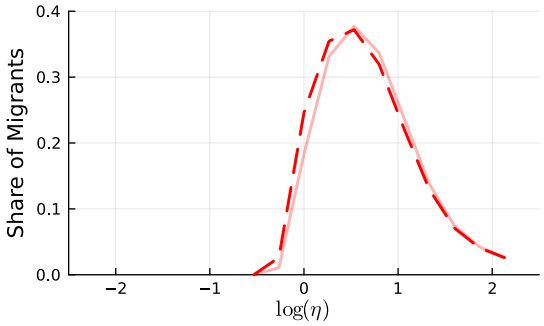

(f) Pessimistic, High-Heat Cash Transfer

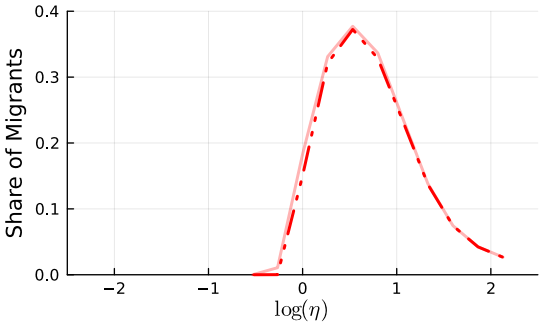

G.3 Probability of Receiving the Transfer

Figure A.13: Probability of Receiving the Transfer

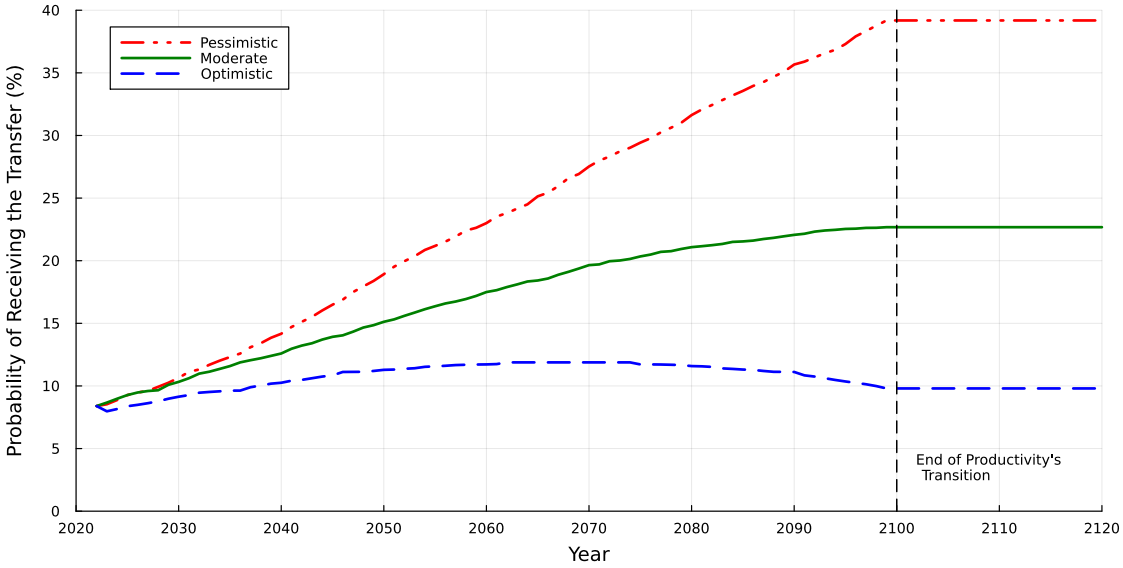

Note: This figure exhibits the probability of an individual receiving the transfer for each scenario over time. In the exercises, we attribute the transfers for individuals that receive a transition shock equal or lower to $\underline{z} = 0.60$. In general, this probability rises over time: the distribution of high heat is changing over time in the direction of high heat becoming more likely, and hence, a lower z becomes more likely.

G.4 Alternative Cash-Transfers Amounts for same UCT schemes

G.4.1 Effect of a 5% Average Income Cash Transfer

Table A.6: Stock of Migrants in the U.S. under different Scenarios and Policies (5% transfer)

Case		2023	2040	2060	2080	2100	2120
Baseline	Optimistic	7.6	8.2	9.2	9.3	8.9	8.8
	Moderate	7.6	8.9	10.8	11.7	12.3	12.5
	Pessimistic	7.6	9.5	13.4	17.1	18.0	16.8
Universal	Optimistic	7.6	8.1	9.0	9.1	8.8	8.6
	Moderate	7.6	8.8	10.6	11.7	12.4	12.6
	Pessimistic	7.6	9.4	13.6	17.3	18.3	17.2
High-Heat	Optimistic	7.6	7.9	8.3	8.2	7.8	7.5
	Moderate	7.6	8.6	10.3	11.1	11.4	11.4
	Pessimistic	7.6	9.3	12.4	16.1	17.4	16.4

Note: This table shows the stock of migrants in the U.S. for the Optimistic, Moderate, and Pessimistic scenarios for our baseline, universal UCT, and High-Heat UCT. Baseline refers to our main results (no cash transfer). Universal refers to the case in which every agent receives a cash transfer. High-Heat refers to the case in which the cash transfer is received only by agents who suffered a drop in productivity of, at least, 40%. he cash transfer used for these exercises is equivalent to 5% of the initial average income.

Table A.7: Annual Cost of the Unconditional Cash Transfers Policies (5% transfer)

Case		2023	2040	2060	2080	2100	2120
Universal	Optimistic	4.1	4.1	4.1	4.1	4.1	4.1
	Moderate	4.1	4.1	4.0	3.9	3.9	3.9
	Pessimistic	4.1	4.1	3.9	3.7	3.7	3.7
High-Heat	Optimistic	0.3	0.4	0.5	0.5	0.4	0.4
	Moderate	0.3	0.5	0.7	0.8	0.9	0.9
	Pessimistic	0.3	0.6	0.9	1.2	1.5	1.5
$\frac{\text{High-Heat}}{\text{Universal}}$ (%)	Optimistic	8.4	10.2	11.8	11.7	9.8	9.8
	Moderate	8.4	12.4	17.1	20.9	22.8	22.9
	Pessimistic	8.4	13.8	22.8	31.7	39.8	39.7

Note: This table shows the cost of the UCTs for the Optimistic, Moderate, and Pessimistic scenarios. In the first two rows, the cost is annual and measured as a percentage of initial average income. The last row indicates the ratio between the cost of the high-heat and the universal cash transfer, expressed in percentages. The cash transfer used for these exercises is equivalent to 5% of the initial average income.

G.4.2 Effect of a 20% Average Income Cash Transfer

Table A.8: Stock of Migrants in the U.S. under different Scenarios and Policies (20% transfer)

Case		2023	2040	2060	2080	2100	2120
Baseline	Optimistic	7.6	8.2	9.2	9.3	8.9	8.8
	Moderate	7.6	8.9	10.8	11.7	12.3	12.5
	Pessimistic	7.6	9.5	13.4	17.1	18.0	16.8
Universal	Optimistic	7.6	7.7	8.4	8.4	8.1	7.9
	Moderate	7.6	8.3	10.3	12.0	13.0	13.2
	Pessimistic	7.6	9.1	14.2	17.7	19.3	18.3
High-Heat	Optimistic	7.6	7.4	6.4	5.7	5.1	4.9
	Moderate	7.6	7.9	7.9	8.7	9.4	9.5
	Pessimistic	7.6	8.5	10.8	12.9	14.4	13.8

Note: This table shows the stock of migrants in the U.S. for the Optimistic, Moderate, and Pessimistic scenarios for our baseline, universal UCT, and High-Heat UCT. Baseline refers to our main results (no cash transfer). Universal refers to the case in which every agent receives a cash transfer. High-Heat refers to the case in which the cash transfer is received only by agents who suffered a drop in productivity of, at least, 40%. he cash transfer used for these exercises is equivalent to 20% of the initial average income.

Table A.9: Annual Cost of the Unconditional Cash Transfers Policies (20% transfer)

Case		2023	2040	2060	2080	2100	2120
Universal	Optimistic	16.5	16.5	16.4	16.4	16.5	16.5
	Moderate	16.5	16.4	16.1	15.8	15.6	15.5
	Pessimistic	16.5	16.3	15.4	14.7	14.4	14.6
High-Heat	Optimistic	1.4	1.7	1.9	1.9	1.6	1.6
	Moderate	1.4	2.0	2.8	3.4	3.7	3.7
	Pessimistic	1.4	2.3	3.6	4.8	6.0	6.1
$\frac{\text{High-Heat}}{\text{Universal}}$ (%)	Optimistic	8.4	10.2	11.9	11.9	10.0	10.0
	Moderate	8.4	12.4	17.6	21.6	23.5	23.6
	Pessimistic	8.4	13.9	23.4	32.6	41.6	41.5

Note: This table shows the cost of the UCTs for the Optimistic, Moderate, and Pessimistic scenarios. In the first two rows, the cost is annual and measured as a percentage of initial average income. The last row indicates the ratio between the cost of the high-heat and the universal cash transfer, expressed in percentages. The cash transfer used for these exercises is equivalent to 20% of the initial average income.

H Interpretation of ν

In the main text, we assume that ν is a multiplicative term to the utility valuation of consumption in the U.S., c^*. In this appendix, we explain in more details this assumption.

Introducing the parameter $\nu > 0$ allows the model more degrees of freedom to match the mass of Migrants that would live in the U.S. Given that the utility function is CRRA,

$$u(c) = \frac{c^{1-\sigma}}{1-\sigma}$$

with $\sigma > 1$. The value of being abroad is given by

$$V^*(\eta) = \frac{u(c^*)\nu + \beta\psi\mathbb{E}_{z'}\left[\mathcal{V}(0,z';\eta)\right]}{1-\beta(1-\psi)}$$

Because the utility level is negative, a higher ν implies a higher disutility of being abroad. We think of this disutility as capturing the non-consumption enjoyment of being away from its mother tongue, different culture, and nourishment, among others.

Ceteris Paribus, a higher level of ν tends to lower the value of emigrating, $V^e(a,z;\eta)$, relative to the value of staying, $V^s(a,z;\eta)$, and avert migration. This results in both a lower mass of migrants and a lower sensitivity of migration probability (or migration rate), the two moments that we target. The more prominent effect tends to be on the mass of migrants, and, in general, ν is much more informative about M than about β_1.

Our estimate for c^* comes directly from the data.[34] An alternative to introducing ν is estimating c^* directly, since there is another level of consumption $\tilde{c}$ such that

$$u(c^*)\nu = u(\tilde{c})$$

which imply

$$\tilde{c} = c^*\nu^{\frac{1}{1-\sigma}}$$

[34] See Section 4.1

Under our parametrization, $\sigma = 2$ and the expression becomes

$$\tilde{c} = \frac{c^*}{\nu}$$

Hence, a larger ν would be equivalent — in terms of utility — to a lower level of consumption. Using $c^* = 4.29\mathbb{E} \times [z]$ and the result from the SMM procedure for ν is 2.58, we find

$$\tilde{c} = \frac{4.29}{2.58} \times \mathbb{E}[z] = 1.66 \times \mathbb{E}[z]$$

The implied valuation of consumption in the U.S. is, therefore, higher than the one of an individual that chooses $q_a a' = a$, conditional on the median productivity $\eta = 1$. In this case, consumption is simply $c^s = wz\eta$ — which occurs if $a = a' = 0$ or $a' - a = a\frac{r}{1+r}$.

In general, the lower the η, the more attractive is $\tilde{c}$ relative to $\mathbb{E}[z]$. Another feature is that c^* is risk-free, while consumption in Guatemala is risky. Thus, the higher the productivity, η, the higher the variance of income and, hence, consumption. So, the higher the η, the feature of c^* being risk-free becomes more attractive to the individual. These two forces that go in opposite directions result in a selection that most migration comes from individuals with $\eta > 1$.

I Identification of Estimated Parameters

In the main text, we approach the quantitative problem by pre-setting some parameters that are readily available in from the data, well-established in the literature or used by reference papers in the literature. We then estimate two parameters using the Simulated Method of Moments, which are the monetary migration cost m^e and the disutility parameter of living in the U.S. ν.

In this appendix, we shed some light on the robustness of our modeling estimates. We show how each parameter we estimate relates to the targeted moments we consider. We start by fixing all pre-set parameters to the ones in the text. Next, we sample pairs of (m^e, ν) and show how each pair relates to the targeted moments. This approach is similar to the one Bilal and Rossi-Hansberg (2023) employ.

We sample 2,500 pairs of the parameters we estimate, (m^e, ν). For each pair, we solve the policy functions and stationary distribution of agents, next sampling cohorts, and finally run a regression in the spirit of Equation 1 for each cohort. We start by specifying an interval that specifies the range of reasonable values for each parameter after some experimentation. The numbers are contained in Table A.10 below.

Table A.10: Interval allowed for each parameter

Parameter	**Lower-bound**	**Upper-bound**
m^e	2.01	2.92
ν	0.00	4.00

Then, we sample 5,000 draws from a normal distribution with zero mean and unitary variance, $N(0,1)$. 2,500 of these draws pin down m^e and 2,500 of these draws pin down ν, making the 2,500 pairs. Equipped with 2,500 pairs of normally distributed sampled variables, we applied the logit transformation explained in Section E of the Appendix, yielding 2,500 pairs of (m^e, ν) that lie in the specified range for each parameter. A desired implication of the use of normality together with the logit transformation is that the sampled points are relatively more concentrated in the centroid of the box.

Given a pair of (m^e, ν) and the remaining parameters, we then solve the stationary distribution and compute the two moments that we target. These two moments are the sensitivity of the migration probability (and therefore migration rates) to the weather shock, β_e, and the stock of Guatemalans in the U.S., M.

Figure A.14: High-heat migration link and stock of migrants in the U.S. by migration cost

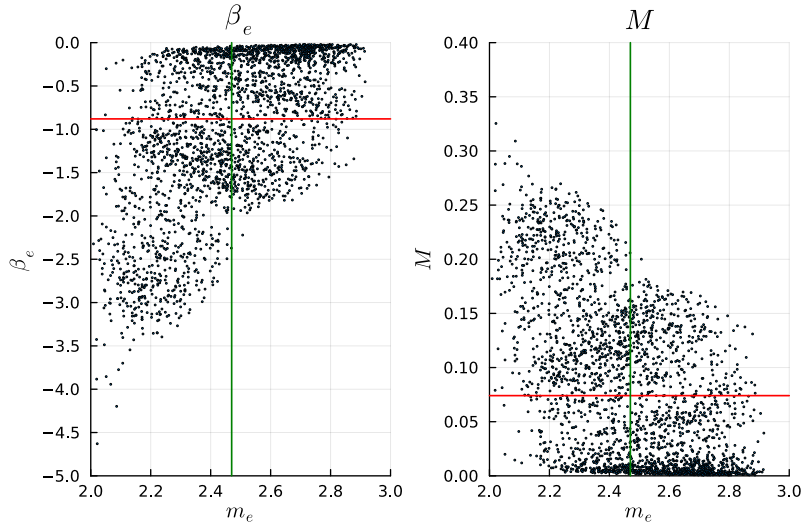

Note: The plot shows 2,500 dots, one for each combination of (m^e, ν), and the respective values of the β_e regression coefficient analogous to the one in Equation (1) and Table 1, in the left panel, and the stock of migrants, M, in the right panel. The horizontal axis shows the value of m^e, while the vertical axis shows the appropriated values for model moments. The horizontal red lines exhibit the target for each moment, while the green vertical line highlights the estimated value for the parameter. Fixing a given level of m^e, the variation observed along the vertical line associated with this level of m^e for each moment (each panel) is driven by different values of ν that was paired with the fixed m^e.

Figure A.15: High-heat migration link and stock of migrants in the U.S. by disutility of living in the U.S.

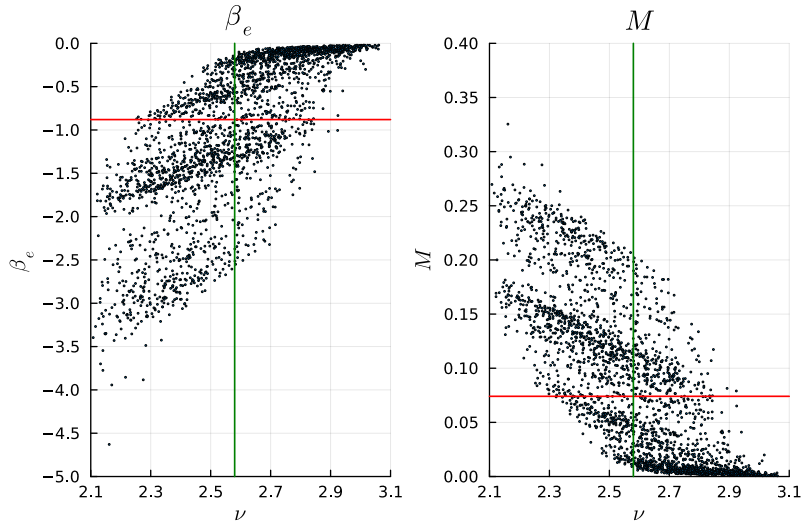

Note: The plot shows 2,500 dots, one for each combination of (m^e, ν), and the respective values of the β_e regression coefficient analogous to the one in Equation (1) and Table 1, in the left panel, and the stock of migrants, M, in the right panel. The horizontal axis shows the value of ν, while the vertical axis shows the appropriated values for model moments. The horizontal red lines exhibit the target for each moment, while the green vertical line highlights the estimated value for the parameter. Fixing a given level of ν, the variation observed along the vertical line associated with this level of ν for each moment (each panel) is driven by different values of m^e that was paired with the fixed ν.

Table A.11: Statistical Description over 2,500 sampled pairs for (m^e, ν)

Symbol	Mean	SD	Min	q25	Median	q75	Max
m^e	2.46	0.21	2.01	2.30	2.47	2.63	2.92
ν	2.58	0.21	2.10	2.42	2.59	2.74	3.06
β_e	-1.03	0.90	-4.63	-1.56	-0.86	-0.19	-0.02
M (%)	8.68	7.53	0.69	1.20	7.60	13.95	32.54

Note: SD stands for standard deviation, Min for minimum, q25 is the 25 percentile, q75 is 75 percentile and Max is the maximum.

Table A.12: Covariance Matrix over 2,500 sampled pairs for (m^e, ν)

Symbol	m^e	ν	β_e	$M(\%)$
m^e	0.04	0.00	0.11	-0.86
ν	0.00	0.05	0.14	-1.26
β_e	0.11	0.14	0.80	-6.74
$M(\%)$	-0.86	-1.26	-6.74	56.75

Note: Numbers are rounded to the second decimal place.

Table A.13: Model's moment and estimated parameters

Variables	(1) β_e	(2) M	(3) m^e	(4) ν
m^e	2.5623***	-0.2014***		-0.0137
	(0.0262)	(0.0020)		(0.0204)
ν	3.1642***	-0.2779***	-0.0131	
	(0.0256)	(0.0019)	(0.0195)	
Observations	2,500	2,500	2,500	2,500
R^2	0.91	0.92	0.00	0.00

Note: Standard errors reported. *** p<0.01, ** p<0.05, * p<0.1.

In column (1) of Table A.13, we run a regression of β_e on m^e, ν, and a constant (not reported). In column (2), we run a similar regression but using M as the dependent variable. Columns (3) and (4) highlight that the draws for m^e and ν are not correlated.

Analyzing the numbers from Tables A.12 and A.13, we observe that, conditional on the values for the pre-set parameters, the parameter controlling the disutility of migration drives a slightly larger share

of the results. While it is true for both moments individually, ν is particularly important for the mass of migrants in the U.S., the importance of m^e is relatively higher for the regression coefficient, β_e.